

SIERPINSKI GASKET PATCH AND MONOPOLE FRACTAL ANTENNA

ABD SHUKUR BIN JA'AFAR

UNIVERSITI TEKNOLOGI MALAYSIA

UNIVERSITI TEKNOLOGI MALAYSIA

BORANG PENGESAHAN STATUS TESIS*

JUDUL: SIERPINSKI GASKET PATCH AND MONOPOLE FRACTAL
ANTENNA

SESI PENGAJIAN: 2004/2005

Saya ABD SHUKUR BIN JA'AFAR

(HURUF BESAR)

mengaku membenarkan tesis (PSM/Sarjana/Doktor Falsafah)* ini disimpan di Perpustakaan Universiti Teknologi Malaysia dengan syarat-syarat kegunaan seperti berikut:

1. Tesis adalah hakmilik Universiti Teknologi Malaysia.
2. Perpustakaan Universiti Teknologi Malaysia dibenarkan membuat salinan untuk tujuan pengajian sahaja.
3. Perpustakaan dibenarkan membuat salinan tesis ini sebagai bahan pertukaran antara institusi pengajian tinggi.
4. **Sila tandakan (✓)

SULIT

(Mengandungi maklumat yang berdarjah keselamatan atau kepentingan Malaysia seperti yang termaktub di dalam AKTA RAHSIA RASMI 1972)

TERHAD

(Mengandungi maklumat TERHAD yang telah ditentukan oleh organisasi/badan di mana penyelidikan dijalankan)

TIDAK TERHAD

Disahkan oleh

(TANDATANGAN PENULIS)

(TANDATANGAN PENYELIA)

Alamat Tetap:

8995, JLN SIDANG MOHD AMIN

KG. TELOK, BUKIT BERUANG,

75450, MELAKA.

DR. MOHAMAD KAMAL BIN A. RAHIM

Nama Penyelia

Tarikh: 04 APRIL 2005

Tarikh: 04 APRIL 2005

- CATATAN:
- * Potong yang tidak berkenaan.
 - ** Jika tesis ini SULIT atau TERHAD, sila lampirkan surat daripada pihak berkuasa/organisasi berkenaan dengan menyatakan sekali sebab dan tempoh tesis ini perlu dikelaskan sebagai SULIT atau TERHAD.
 - ◆ Tesis dimaksudkan sebagai tesis bagi Ijazah Doktor Falsafah dan Sarjana secara penyelidikan, atau disertasi bagi pengajian secara kerja kursus dan penyelidikan, atau Laporan Projek Sarjana Muda (PSM).

“I declare that I have read this thesis and in my opinion,
it is suitable in terms of scope and quality for the purpose of
awarding a master degree in Electrical Engineering”.

Signature : _____
Supervisor : Dr. Mohamad Kamal Bin A. Rahim
Date : 04 April 2005

SIERPINSKI GASKET PATCH AND MONOPOLE ANTENNA

ABD SHUKUR BIN JA'AFAR

**A thesis submitted in fulfilment
of the requirements for the award of the
Degree of Master of Engineering
(Electrical-Electronics & Telecommunications)**

**Faculty of Electrical Engineering
Universiti Teknologi Malaysia**

MARCH 2005

DECLARATION

“ I hereby declare that the materials presented in this thesis are the result of my own work except as cited as reference. The thesis has not been accepted for any degree and is not concurrently submitted in candidature of any degree.”

Signature :

Name : Abd Shukur Bin Ja'afar

Date : 04 April 2005

To My Loving and Caring Family ...

ACKNOWLEDGEMENTS

My first thanks is for my supervisor, Dr. Mohamad Kamal A. Rahim, whose constant support, patience and unbounded enthusiasm were of invaluable help. His devotion to the needs of the students and the encouragements has made working with him a true delight.

My sincere appreciation to my fellow colleagues in the sharing the similar research interests. I value the camaraderie we share as well as the time they spent to share with me enriching ideas, as well as their concern. My gratitude especially goes to Lester Cheung, Mohd Zoinol, Azahari, Abd Hafizh, Mohd Fairus Yusof, and Asrul Izzam for many hours of discussions, as well as assistance during fabrication process.

My sincerest thanks to all those who have helped to make this thesis possible. Warmest regards to my mother, sister, both grandmother and grandfather for their seamless caring encouragement and moral support that has made this journey possible.

ABSTRACT

The use of fractal geometry in designing antenna has been a recent topic of interest. It has already proved that fractal shaped have their own unique characteristics that improved antenna achievement without degrading antenna properties. This dissertation tells about one of familiar geometry in fractal antenna, Sierpinski gasket. Here, two types of antenna are designed: Sierpinski gasket patch and Sierpinski gasket monopole. Maximum iteration that applies to these antennas is three. The behaviors of both type antennas are investigated such as return loss, number of iteration and radiation pattern. Simulation, fabrication and testing have been done. The entire antenna shows multiband in resonant frequencies. For Sierpinski monopole shows a pattern in return loss but not for Sierpinski patch. Monopole type shows the frequency band log-periodically spaced by two, same as the scale factor among the structure (sub-gasket). The self-similarity properties of fractal structure are translated into its electromagnetic behavior.

ABSTRAK

Penggunaan geometri *fractal* di dalam rekabentuk antenna menjadi satu tumpuan sejak kebelakangan ini. Kajian telah membuktikan rekabentuk *fractal* mempunyai sifat yang unik di mana ia membantu pencapaian sesuatu antenna tanpa mngurangkan prestasi asal. Disetasi ini membincangkan mengenai salah satu rekabentuk *fractal* yang terkenal iaitu Sierpinski gasket. Di sini, dua jenis antenna direkabentuk berdasarkan geometri Sierpinski gasket iaitu mikrojalur (antena tampal) dan ekakutub. Antenna tersebut disegmenkan sehingga iterasi ketiga. Kelakuan antenna fractal ini dikaji dari segi perubahan kehilangan kembali, bilangan iterasi yang dilaksanakan, dan corak sinaran. Simulasi, fabrikasi dan pengukuran telah dilaksanakan. Kesemua antenna menunjukkan sifat multijalur frekuensi apabila *fractal* dilaksanakan. Bagi jenis ekakutub, kehilangan kembali mempamerkan corak yang boleh dijangka tetapi tidak pada jenis mikrojalur. Jenis ekakutub juga menunjukkan pengulangan berkala jalur frekuensi sebanyak 2 kali ganda, dimana boleh diakitkan dengan struktur rekabentuk gasket antenna tersebut. Ini boleh dikatakan rekabentuk kesamaan pada antenna tersebut di pindahkan ke kelakuan elektromagnetiknya.

TABLE OF CONTENTS

CHAPTER	TITLE	PAGE
	TITLE	i
	DECLARATION	ii
	DEDICATION	iii
	ACKNOWLEDGEMENTS	iv
	ABSTRACT	v
	ABSTRAK	vi
	TABLE OF CONTENTS	vii
	LIST OF TABLES	x
	LIST OF FIGURES	xi
	LIST OF SYMBOLS	xiii
	LIST OF APPENDICES	xiv
	LIST OF ABBREVIATIONS	xv
CHAPTER 1	INTRODUCTION	1
	1.1 Project Background	1
	1.2 Objective	2
	1.3 Scope of Projects	2
	1.4 Project Methodology	3
	1.5 Thesis Outlines	4

CHAPTER 2	ANTENNA THEORY	6
2.1	Introduction	6
2.2	Antenna Properties	7
2.2.1	Input Impedance	7
2.2.2	VSWR	7
2.2.3	Gain	9
2.2.4	Radiation Pattern	9
2.2.5	3dB Beamwidth (HPBW)	11
2.2.6	Directivity	11
2.2.7	Polarization	12
2.2.8	Bandwidth	12
2.3	Scattering Parameters	13
2.4	Basic Microstrip Antennas	15
2.5	Analysis of Microstrip Antennas	17
2.5.1	Transmission Line Model	18
2.5.2	Full Wave Analysis	20
2.5.3	Cavity Model	20
2.5.3.1	Equilateral Triangle Microstrip Antenna	21
2.5.3.2	Resonant Frequency	22
2.6	Feeding Techniques	23
2.6.1	Coaxial Probe Feed	23
2.6.2	Side Feed	24
2.7	Matching Techniques	25
2.8	Summary	27
CHAPTER 3	FRACTAL ANTENNA	28

3.1	Fractal Background	28
3.2	Fractal Antenna Elements	31
3.3	Fractal Geometry	32
	3.3.1 Sierpinski Carpet	33
	3.3.2 Koch curves	33
	3.3.3 Hilbert curves	34
3.4	Sierpinski Gasket Geometry	35
	3.4.1 Generation of Sierpinski Gasket Geometry	36
3.5	Sierpinski Gasket Monopole	39
3.6	Design Procedure	40
	3.6.1 Sierpinski Gasket Patch	43
	3.6.2 Sierpinski Gasket Monopole	45
3.7	Summary	47
CHAPTER 4	SIMULATION, FABRICATION AND MEASUREMENT	48
4.1	Introduction	48
4.2	Fabrication	52
	4.2.1 Etching Process	52
	4.2.2 Connector	53
4.3	Antenna Measurement	56
4.4	Summary	57
CHAPTER 5	rESULTS AND DISCUSSIONS	58
5.1	Introduction	58
5.2	Simulation Result	58

5.3	Measurement Result	68
5.4	Summary	77
CHAPTER 6	CONCLUSION AND RECOMMENDATION	78
7.1	Introduction	78
7.2	Conclusion	78
7.3	Recommendations And Future Works	79
REFERENCES		80
APPENDIX A		86
APPENDIX B		88
APPENDIX C		90
APPENDIX D		92
APPENDIX E		96

LIST OF TABLES

TABLE	DESCRIPTION	PAGE
2.1	VSWR vs return loss	8
3.1	Laminates Specifications	41
3.2	Dimension for the antennas	43
3.3	SGFm2 geometry parameters	46
5.1	Frequency band, return loss and bandwidth	59
5.2	Frequency band, return loss and bandwidth	60
5.3	Frequency band, return loss and bandwidth	60
5.4	Frequency band, return loss and bandwidth	61
5.5	Frequency band, return loss and bandwidth	62
5.6	Frequency band, return loss and bandwidth	63
5.7	Frequency band, return loss and bandwidth for measurement	69
5.8	Frequency band, return loss and bandwidth for measurement	70
5.9	Frequency band, return loss and bandwidth for measurement	72
5.10	Frequency band, return loss and bandwidth for measurement	74

LIST OF FIGURES

FIGURE	DESCRIPTION	PAGE
1.1	Geometry of each design antenna	4
2.1	Example of radiation pattern	10
2.2	Convention used to define S-parameters for a two-port network	14
2.3	Basic structure of microstrip antenna	16
2.4	Charge distribution and current density	16
2.5	Transmission line model of microstrip antenna	18
2.6	Cavity model of patch antenna	21
2.7	Structure antenna with coaxial probe feeding technique	24
2.8	Antenna structure with side feed microstrip line	25
2.9	Matching with single section quarter wave transformer	26
3.1	Example geometry in nature that is modeled using fractal-fern	30
3.2	Example geometry in nature that is modeled using fractal-landscape	30
3.3	Example fractal geometry in nature	31
3.4	Example of fractal antenna	32
3.5	Four stages in construction of Sierpinski carpet	33
3.6	Step of construction of Koch curves geometries	34
3.7	Four stage in construction of Hilbert curves	35
3.8	Multiple copy generation approach	37

3.9	Decomposition generation approach	37
3.10	Iterated Function System for generation of self-similar Sierpinski gasket geometry	38
3.11	Sierpinski gasket monopole antenna	39
3.12	Flow chart of the design procedure for SGFpe1, SGFpd1, and SGFm1	42
3.13	Stage of construct Sierpinski gasket patch	44
3.14	Introducing coupling patches-SGFpe1 and SGFpd1	45
3.15	Dimension of SGFm2	46
4.1	Microwave Office Environment	49
4.2	TXLINE calculator	49
4.3	Layout design on EM structure	50
4.4	3D view of layout design	51
4.5	Types of connector that are used	53
4.6	Step of fabrication process from beginning to measurement	54
4.7	Sierpinski gasket patch antenna	55
4.8	Sierpinski gasket monopole antenna	55
4.9	Radiation pattern measurement setup	57
5.1	Return loss response of SGFpe1 at 1 st iteration	59
5.2	Return loss response of SGFpe1 at 2nd iteration	59
5.3	Return loss response of SGFpe1 at 3rd iteration	60
5.4	Return loss response of SGFpd1 at 1st iteration	61
5.5	Return loss response of SGFpd1 at 2nd iteration	62
5.6	Return loss response of SGFpd1 at 3 rd iteration	63
5.7	Radiation pattern simulation at $\Phi=0$ cut (E-plane) for SGFpe1	64
5.8	Radiation pattern simulation at $\Phi=90$ cut (H-plane) for SGFpe1	65
5.9	Radiation pattern simulation at $\Phi=0$ (E-plane) for SGFpd1	66
5.10	Radiation pattern simulation at $\Phi=90$ (H-plane) for SGFpd1	67
5.11	Comparison simulation and measurement of SGFpd1 antenna	68
5.12	Comparison simulation and measurement of SGFpe1 antenna.	69
5.13	Measurement plot of co-polarisation and	

	cross-polarisation for SGFpd1	71
5.14	Return loss measurement for SGFm1 antenna	72
5.15	Measurement plot of co-polarisation and cross-polarisation for SGFm1	73
5.16	Return loss measurement for SGFm2 antenna	74
5.17	Measurement plot of co-polarisation and cross-polarisation for SGFm2	76

LIST OF SYMBOLS

BW	-	Bandwidth
c	-	Velocity of light
D	-	Directivity
f	-	Frequency
f_o	-	Operating frequency
f_r	-	Resonant frequency
G	-	Gain
h	-	Substrates thickness
S_{11}	-	Return loss
t	-	Thickness of conductor
$\tan\delta$	-	Loss tangent
VSWR	-	Voltage standing wave ratio
w	-	Width of feed line
Z_{in}	-	Input impedance.
Z_o	-	Characteristic impedance
Z_L	-	Load impedance
ϵ_r	-	Relative permittivity
ϵ_{eff}	-	Effective relative permittivity
σ	-	Conductivity
λ_o	-	Free space wavelength
λ_g	-	Guided wavelength
π	-	3.142

η - Efficiency

LIST OF APPENDICES

APPENDIX	DESCRIPTION	PAGE
Appendix A	Transmission lines width calculation-Mathcad2000	86
Appendix B	Calculating dimension a of triangle	88
Appendix C	Figure of return loss for all iteration	90
Appendix D	Equipment for measurement and fabricated antenna	92
Appendix E	Example of MATLAB program to plot radiation pattern.	96

LIST OF ABBREVIATIONS

	SGFpe1	SGFpd1	SGFm1	SGFm2	
S	-				Sierpinski
G	-				Gasket
F	-				Fractal
p	-				patch
m	-				monopole
e	-				edge feed
d	-				direct feed
#	-				version number

RF	-	Radio Frequency
VSWR	-	Voltage Standing Wave Ratio
HPBW	-	Half Power Beamwidth
dB	-	decibel

CHAPTER 1

INTRODUCTION

1.1 Project Background

In modern wireless communication systems and increasing of other wireless applications, wider bandwidth, multiband and low profile antennas are in great demand for both commercial and military applications. This has initiated antenna research in various directions, one of them is using fractal shaped antenna elements. Traditionally, each antenna operates at a single or dual frequency bands, where different antenna is needed for different applications. This will cause a limited space and place problem. In order to overcome this problem, multiband antenna can be used where a single antenna can operate at many frequency bands. One technique to construct a multiband antenna is by applying fractal shape into antenna geometry.

This project presents the Sierpinski gasket patch and monopole antenna where this famous shape, the antenna behaviors are investigated. In addition to the theoretical design procedure, numerical simulation was performed using Moment of Methods

(Mom) software (Microwave Office, ADS) to obtain design parameters such as size of patch and feeding location. The antennas have been fabricated and tested.

1.2 Objective

The objective of this project is to design, simulate and fabricate the Sierpinski gasket patch (microstrip) and monopole fractal antenna. The behavior and properties of these antennas are investigated.

1.3 Scope of Project

The scopes defined for this project are as follows:

- Understanding the antenna concept.
- Design the equilateral triangle for microstrip at 1.8GHz, and fractal it until 3rd iteration. The same structure will be used for monopole type.
- Performs numerical solution using Microwave Office V6 and Advance Design System (ADS) softwares.
- Practical implementation of the antennas.
- Measurement of the antennas properties.
- Comparison the measurement and simulation results.

1.4 Project Methodology

The project begins with the understanding of the microstrip antenna technology. This includes the property studies such as the radiation pattern, input impedance and operating frequency. The related literature reviews includes understanding the Sierpinski gasket shape for monopole type. The design of the microstrip Sierpinski gasket starts with an equilateral triangle as an initiator with operating frequency at 1.8 GHz. This will determine the size of the patch before iteration need to apply. The next step is to choose the relevant material such as microwave laminate. The information is used to calculate the characteristics and performance of the antenna. The software used for numerical simulation are Microwave Office V6 and Advance Design System (ADS). The practical implementation is carried out after the simulation process. This involves the artwork preparation for the antenna fabrication as well as connecting the appropriate connector. The knowledge of AutoCAD software is very useful in fulfilling this task. AutoCAD software is chosen to print actual antenna size on transparency for fabrication process. Then the measurement was performed. Comparisons between simulation and experimental results are made.

In this project four antennas have been fabricated. For Sierpinski gasket patch two variations of feeding techniques have been constructed, which is the direct feed and the edge feed. The antennas are named as SGFdf1, SGFef1, SGFm1, and SGFm2. Figure 1.1 shows the geometry of each antenna.

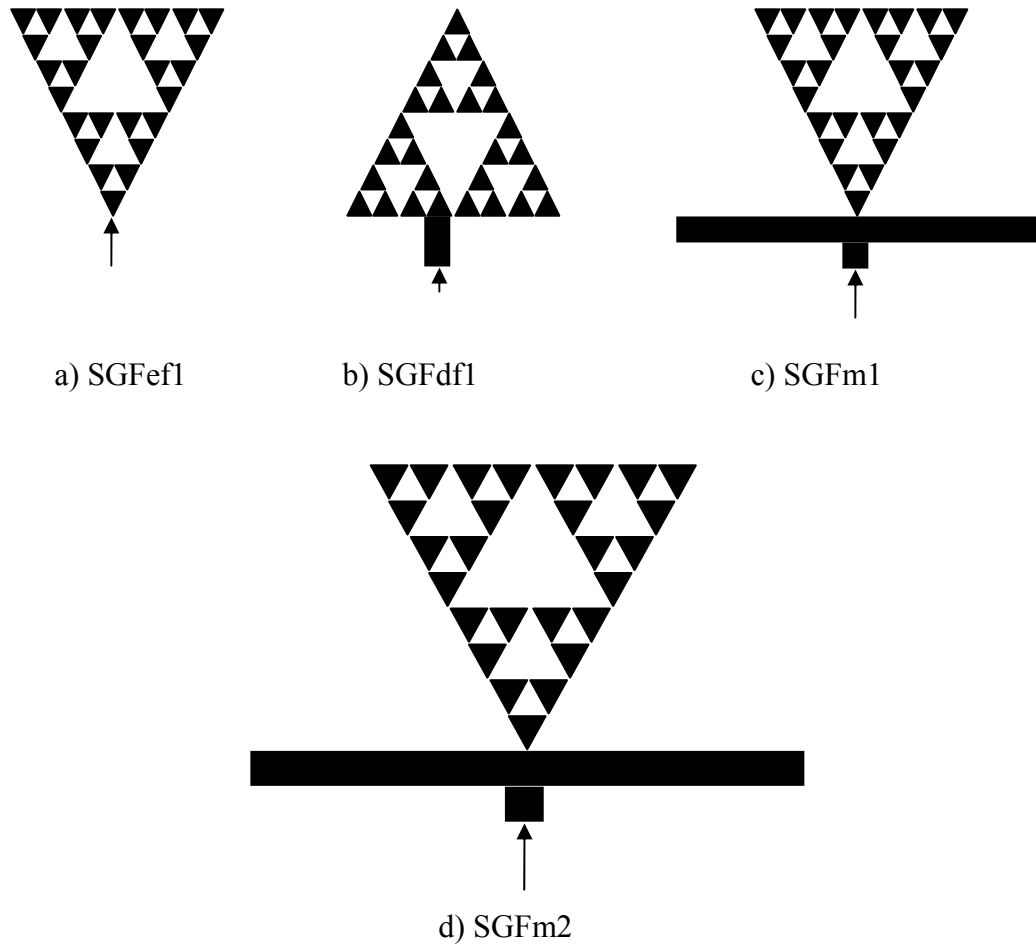


Figure 1.1: Geometry of each antenna.

1.5 Thesis Outline

The thesis is organized into 7 chapters. Chapter 1 presents the overall idea of this thesis including objective, scope of project and project methodology. Chapter 2 presents basic theory antenna theory and properties.

Chapter 3 presents the background or the idea of fractals dimension. The geometry of Sierpinski gasket also has been elaborate here.

Chapter 5 tells about simulation software, fabrication process and testing of the antennas. Chapter 6 presents the result and discussion in detail. The final chapter, Chapter 7 emphasizes on conclusion, recommendations and future works.

CHAPTER 2

ANTENNA THEORY

2.1 Introduction

Microstrip antenna was a simple antenna that consists of radiated patch component, dielectric substrate, and ground plane. The radiated patch and ground plane is a thin layer of cuprum or gold which is good conductor. Each dielectric substrate has their own dielectric permittivity value. This permittivity will influence the size of the antenna. Microstrip antenna is a low profile antenna. They have several advantages like light, small dimension, cheap and easily to integrate with other circuit make it is chosen in many applications.

2.2 Antenna Properties

The performance of the antenna is determined by several factors that also called antenna properties as follows:

2.2.1 Input Impedance

Generally, input impedance is important to determine maximum power transfer between transmission line and the antenna. This transfer only happen when input impedance of antenna and input impedance of the transmission line are match. If not match, reflected wave will be generated at the antenna terminal and travel back towards the energy source. This reflection of energy results causes a reduction in the overall system efficiency. If the return loss is known, the input impedance is given by

$$Z_{in} = Z_0 \left(\frac{1 + S_{11}}{1 - S_{11}} \right) \quad (2.1)$$

2.2.2 VSWR


Voltage Standing Wave Ratio (VSWR) is the ratio between the maximum voltage and the minimum voltage along transmission line. The VSWR, which can derived from the level of reflected and incident waves, is also an indication of how

closely or efficiently an antenna's terminal input impedance is matched to the characteristic impedance of the transmission line. Increasing in VSWR indicates an increase in the mismatch between the antenna and the transmission line. A decrease VSWR means good matching with minimum VSWR is one. The VSWR is given by

$$VSWR = \frac{1 + S_{11}}{1 - S_{11}} \quad (2.2)$$

Most wireless system operates at 50 Ohm impedance. Hence the antenna must be designed with an impedance as close to 50 ohm as possible. A VSWR of 1 indicate an antenna impedance of exactly 50 ohms. Mostly, the ratio of $VSWR \geq 1.5:1$ is needed for antenna functional. Table 1.0 shows several VSWR value compare to reflection coefficient $[S_{11}]$ value. Value of VSWR 2:1 ($[S_{11}] = -9.5$ dB) shows 90% of power reflected. While for VSWR 3:1 ($[S_{11}] = -6$ dB), shows 75 % power is reflected. A good antenna to operate is within $1 \leq VSWR \leq 2$.

Table 2.1: VSWR vs return loss.

	VSWR	Return Loss $[S_{11}]$
 <p>Good</p> <p>Not Good</p>	1.01	-46.1
	1.05	-32.3
	1.10	-26.4
	1.20	-20.8
	1.30	-17.7
	1.40	-15.6
	1.50	-14.0
	1.75	-11.3
	2.00	-9.5
	2.50	-7.4
	3.01	-6.0

2.2.3 Gain

The gain of an antenna is essentially a measure of the antenna's overall efficiency. If an antenna is 100% efficient, it would have a gain equal to its directivity. There are many factors that affect and reduce at the overall efficiency of an antenna. Some of the most significant factors that impact antenna gain include impedance, matching network losses, material losses and radome losses. By considering of all factor, it would appear that the antenna must overcome a lot of adversity in order to achieve acceptable gain performance. Gain is given by (32)

$$G = \frac{|S_{12}| \left(\frac{4\pi d}{\lambda_0} \right)}{\sqrt{(1 - |S_{11}|^2)(1 - |S_{22}|^2)}} \quad (2.3)$$

where d is distance between the transmitting and receiving antenna. Gain also can be simply defined as the product of the directivity and efficiency given by [3]

$$G = \eta D \quad (2.4)$$

2.2.4 Radiation Pattern

The radiation patterns of an antenna provide the information that describes how the antenna directs the energy it radiates. All antennas, if 100% efficient, will radiate the same total energy for equal input power regardless of pattern shape. Radiation patterns are generally presented on a relative power dB scale. It can be show in polar

plot 360 degree. Example of radiation pattern is shown in Figure 3.3. In many cases, the convention of an E-plane and H-plane pattern is used in the presentation of antenna pattern data. The E-plane is the plane that contains the antenna's radiated electric field potential while the H-plane is the plane that contains the antenna's radiated magnetic field potential. These planes are always orthogonal.

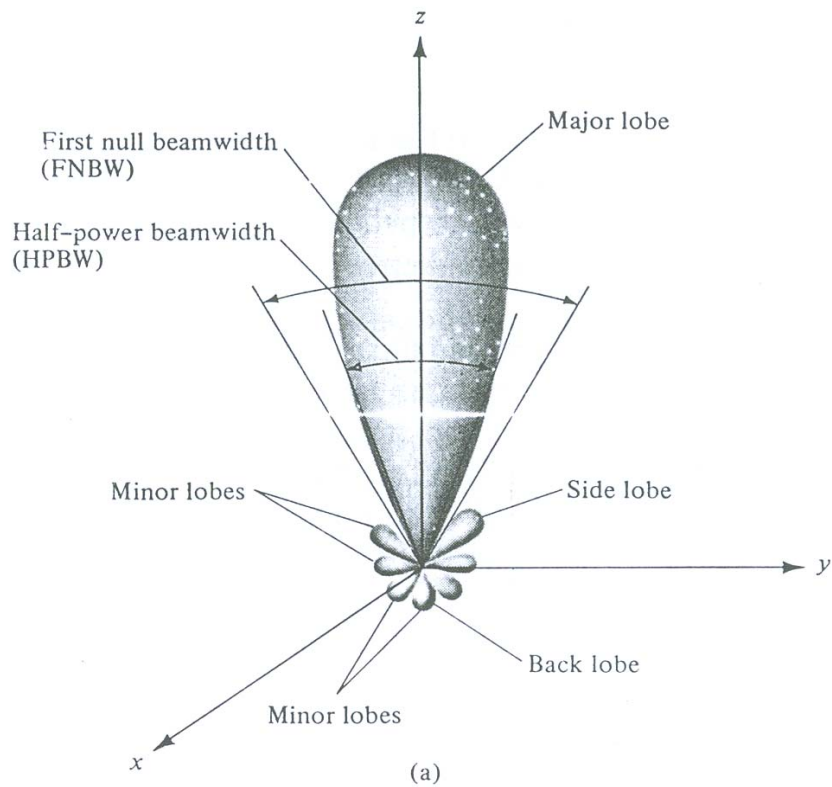


Figure 2.1: Example of radiation pattern [3].

2.2.5 3 dB Beamwidth (half power beam width, HPBW)

Once the antenna pattern information is detailed in a polar plot, some quantitative aspects of the antenna pattern properties can be described. These quantitative aspects include the 3 dB beamwidth (1/2 power level), directivity, side lobe level and front to back ratio. To further understand these concepts, first consider the fundamental reference antenna, the point source. A point source is an imaginary antenna that radiates energy equally in all directions such that the antenna pattern is perfect sphere. These antennas is said to be an omnidirectional isotropic radiator and has 0 dB directivity. In practice when antenna is said to be an omnidirectional, it is inferred that this is referenced only to the horizontal or azimuth sweep plane. For any practical the 3 dB beamwidth of antenna is simply a measure of the angular width of the -3dB points on the antenna pattern relative to the pattern maximum. These -3dB points on the pattern represent the point on the pattern where the power level is down 3 dB of the value at the pattern maximum. Generally, the 3 dB beamwidth is expressed separately for each of the individual pattern sweep planes antenna, there will always be some specific direction of maximum radiated energy.

2.2.6 Directivity

Directivity, D , is important parameter that shows the ability of the antenna focusing radiated energy. Directivity is the ratio of maximum radiated to radiate reference antenna. Reference antenna usually is a isotropic radiator where the radiated energy are same in all direction and have directivity of 1. Directivity can be definition as

$$D = \frac{F_{\max}}{F_o} \quad (2.5)$$

where F_{\max} = maximum radiated energy
 F_o = isotropic radiator radiated energy

2.2.7 Polarization

The polarization of an antenna describes the orientation and sense of the radiated wave's electric field vector. There are three types of basic polarization:

- linear polarization (linear)
- elliptical polarization
- circular polarization

Generally most antennas radiated with linear or circular polarization. Antennas with linear polarization radiated at the same plane with the direction of the wave propagate. For circular polarization, the antenna radiated in circular form.

2.2.8 Bandwidth, BW

The term bandwidth simply defines the frequency range over which an antenna meets a certain set of specification performance criteria. The important issue to consider regarding bandwidth is the performance tradeoffs between all of the performance

properties described above. There are two methods for computing an antenna bandwidth. An antenna is considered broadband if $f_H/f_L \geq 2$.

Narrowband by %

$$BW_p = \frac{f_H - f_L}{f_o} \times 100 \% \quad (2.5)$$

Broadband by ratio

$$BW_b = \frac{f_H}{f_L} \quad (2.6)$$

where $f_o \equiv$ operating frequency

$f_H \equiv$ higher cut-off frequency

$f_L \equiv$ lower cut-off frequency

2.3 Scattering Parameters

When designing RF or Microwave systems, the scattering / S-parameter representations plays a central role. System characterization can no longer be accomplished through simple open or short circuit measurements for high frequencies. This is because of the wire itself possess an inductance that can be of substantial magnitude at high frequency when we short circuit it, while open circuit leads to capacitive loading at the terminal.

S-parameter are power wave descriptors that define input-output relations of a network in terms of incident and reflected power waves.

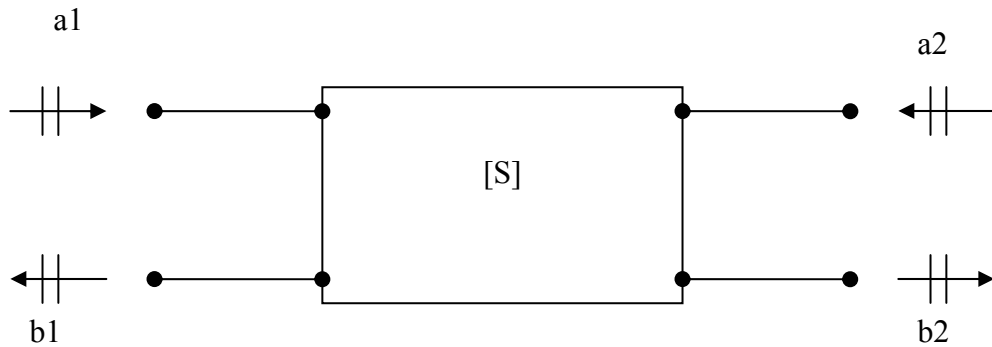


Figure 2.2: Convention used to define S-parameters for a two-port network.

Based on the directional convention shown in figure above, the position to define the S-parameters:

$$\begin{Bmatrix} b_1 \\ b_2 \end{Bmatrix} = \begin{bmatrix} S_{11} & S_{12} \\ S_{21} & S_{22} \end{bmatrix} \begin{Bmatrix} a_1 \\ a_2 \end{Bmatrix} \quad (2.7)$$

where the terms are:

S_{11} is the electric field leaving the input divided by the electric field entering the input, under the condition that no signal enters the output. Since b_1 and a_1 are the electric fields, their ratio is a reflection coefficient.

$$S_{11} = \frac{b_1}{a_1} \text{ when } a_2=0 \quad \begin{array}{l} \text{reflected power wave at port1/incident power wave at} \\ \text{port1} \end{array}$$

S_{21} is term the transmission coefficient related which the electric field is leaving the output divided by the electric field entering the input, when no signal enters the output.

$$S_{21} = \frac{b_2}{a_1} \text{ when } a_2=0 \quad \text{transmitted power wave at port 2/incident power wave at port 1.}$$

S_{12} is a transmission coefficient related to the isolation of the component and specifies how much power leaks back through the component in the wrong direction.

$$S_{12} = \frac{b_1}{a_2} \text{ when } a_1=0 \quad \text{transmitted power wave at port 1/ incident power wave at port 2}$$

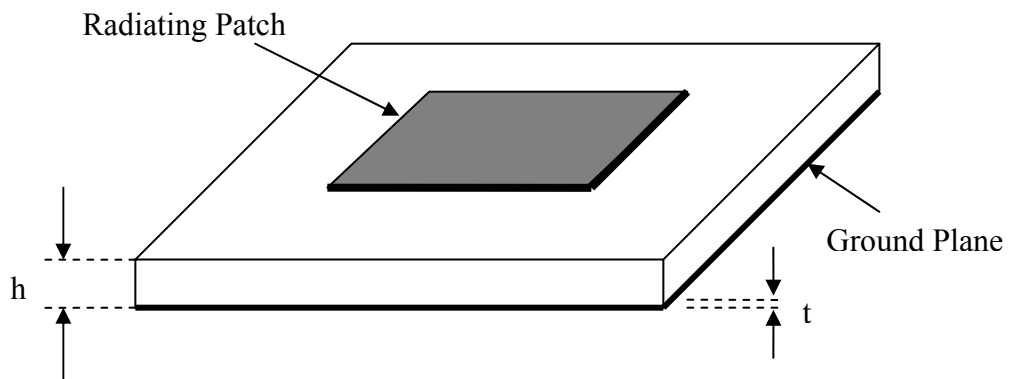
S_{22} is similar to S_{11} but looks in the other direction into the component.

$$S_{22} = \frac{b_2}{a_2} \text{ when } a_1=0 \quad \text{reflected power wave at port 2/ incident power wave at port 2}$$

2.4 Basic Microstrip Antenna

The first idea to use microstrip antenna begin since beginning of 1950's and design concept introduce by Deschamps[15]. Several years later, Gutton and Baissinot have patent the basic microstrip antenna. It was first published in 1952 by Grieg and Englemann [16].

Figure 2.3 show the basic structure of microstrip antenna which consists of radiating patch, dielectric substrates and ground plane. Bottom layer of dielectric substrate is fully covered by conductors that act as a ground plane. The thickness of substrates layer can increase the bandwidth and efficiency, but unfortunately it will generate surface wave with low propagation that cause lost of power.



$h \equiv$ substrates thickness

$t \equiv$ conductor thickness

Figure 2.3: Basic structure of microstrip antenna.

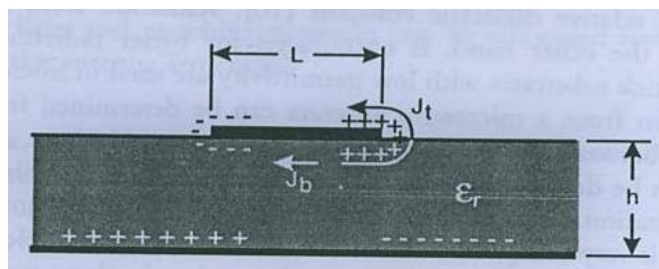


Figure 2.4: Charge distribution and current density on a microstrip antenna [2].

Figure 2.4 shows a charge distribution and current density on a microstrip antenna. When a microstrip antenna is connected to a microwave source, it is energized. The charge distribution will establish on the upper and lower surfaces of the patch, as well as

on the surface on the ground plane. The positive and negative charge distribution then arises. For more detail about further discussion can refer to [2].

Microstrip antennas have got high intention because of their good characteristics like:

- Low profile
- Light
- Cheap
- Easily to integrate with other circuit
- Can be used widely in many applications both in commercial or military.
- Not needed complicated part.

However there are several weaknesses or disadvantages of using microstrip antennas:

- Narrow bandwidth
- Low gain
- Surface wave excitation
- Low efficiency
- Low power handling capacity

2.5 Analysis of Microstrip Antenna.

There are several approach to analyze microstrip antenna. Among the favorite are transmission line, cavity model, and full-wave analysis. Transmission line model are the simple way of analysis. It gives goof interior behavior even though less precisely. But it is good enough to give good result. Compare to cavity model it is more difficult to realize, but it will give a better result. The most precisely method for analysis is full-wave model, but it need to go through difficult process.

2.5.1 Transmission Lines Model

In this model, the interior region of the patch can be modeled as a section of transmission line. Figure 2.5 shows the rectangular patch with its equivalent circuit model. The most significant contribution to broadside radiation comes from the two non resonant ends, appropriately termed the radiating edges. The edge of resonant length also known as non-radiating edges or ends.

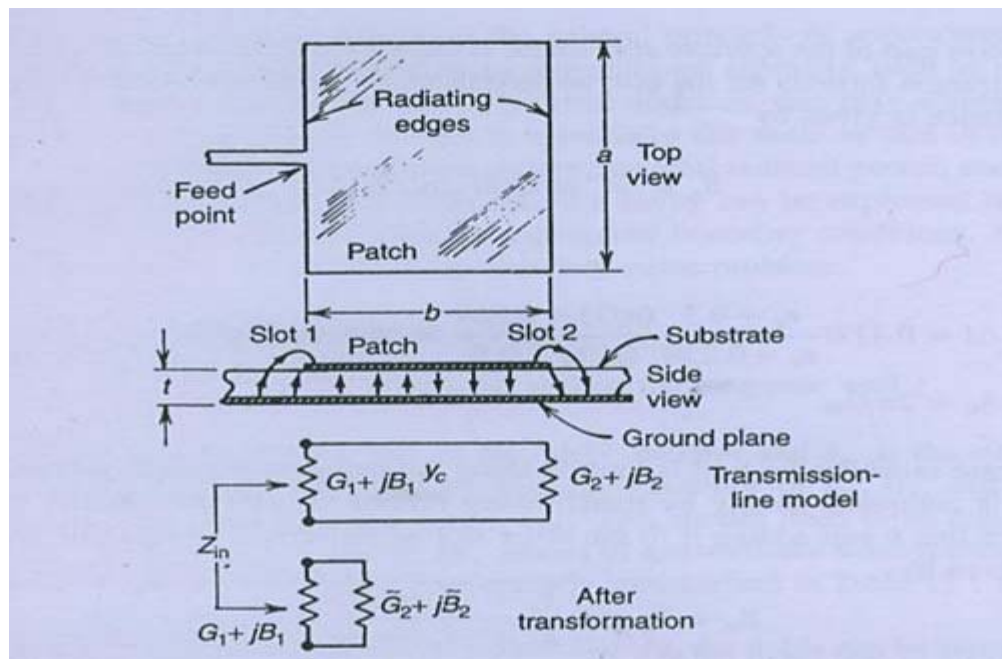


Figure 2.5: Transmission line model of rectangular patch antenna [20].

The radiating edges are treated as slots with dimensions a , t , having constant electric field aperture distributions. The characteristic impedance of the microstrip line (Z_c) can be express as follows:

$$Z_c = \frac{Z_o}{\sqrt{\epsilon_e}} \frac{t}{a} \quad t/a \ll 1$$

where

$$\varepsilon_e = \frac{\varepsilon_r + 1}{2} + \frac{\varepsilon_r - 1}{2} \left(1 + \frac{12t}{a}\right)^{-1/2}$$

$Z_0 = 120\pi$ = free space impedance

ε_r = relative permittivity of substrates

t = substrates thickness

For case which the feed is located along the radiating edge, the equation for Y_{in} is given by [20]:

$$Y_{in} = Y_a + Y_c \frac{Y_a + jY_c \tan \beta b}{Y_c + jY_a \tan \beta b}$$

where $Y_a = G_a + jB_a$ = aperture admittance

$\beta = (2\pi / \lambda_o) \sqrt{\varepsilon_e}$ = transmission line propagation constant

At resonance, further manipulation to the equation gives:

$$(b + 2\Delta l) f_r = c / (2\sqrt{\varepsilon_e})$$

where f_r is the resonance frequency and c is the speed of light in vacuum. Further details can refer to [20].

2.5.2 Full Wave Analysis

There are three popular techniques for full-wave analysis. These are called the *spectral domain full-wave solution*, the *mixed-potential electric field integral equation approach*, and *finite-difference time-domain* technique. Some of the features of the full-wave techniques include:

- Accuracy – This technique provide the most accurate solution.
- Versatility – It can be used for arbitrarily shaped of microstrip elements including multilayer geometries, and various types of feeding techniques.
- Completeness – The solutions include the effects of dielectric and conductor loss, space wave radiation, surfaces wave and coupling effects.
- Computation cost – Numerical method is used in full-wave techniques, therefore require careful programming to reduce computation cost.

2.5.3 Cavity Model

Microstrip patch antennas can be termed lossy cavities. Therefore cavity model becomes a natural choice to analyze patch antennas. In this model, the interior region of the patch is modeled as a cavity bounded by electric walls on the top and bottom, and magnetic wall all along the periphery. This assumption only for thin substrates ($h \ll \lambda_0$):

- The field in the interior region do not vary with z (that is $\delta / \delta z = 0$) because the substrate is very thin, $g \ll \lambda_0$.

- The electric field is z directed only, and the magnetic field has only the transverse components in the region bounded by the patch metallization and the ground plane. This observation provides for the electric walls at the top and bottom.
- The electric current in the patch has no component normal to the edge of the patch metallization, which implies that the tangential component of H along the edge is negligible, and a magnetic wall can be placed along the periphery. Mathematically, $\delta E_z / \delta n = 0$. for more detail about this analysis, can refer to [2].

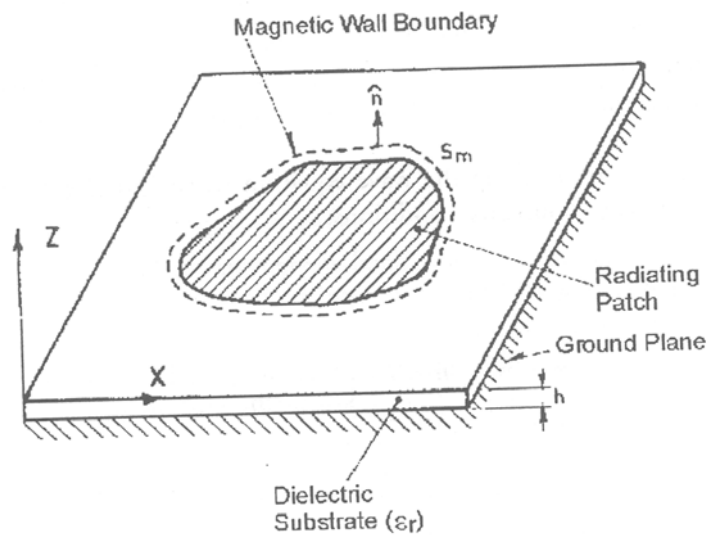


Figure 2.6: Cavity model of a microstrip patch antenna [2].

2.5.3.1 Equilateral Triangular Microstrip Antenna.

Triangular patch antennas have been studied both theoretically and experimentally. They are found to provide radiation characteristics similar to those of rectangular patches, but with smaller size. The simplest of the triangular shapes, it comprises an equilateral triangular conductor on a ground dielectric substrate.

2.5.3.2 Resonant Frequency

The resonant frequency corresponding to the various modes described by k_{mn} [2] is:

$$fr = \frac{ck_{mn}}{2\pi\sqrt{\epsilon_r}} = \frac{2c}{3a\sqrt{\epsilon_r}} \sqrt{m^2 + mn + n^2} \quad (2.8)$$

Here c is the velocity of light in free space. The above formula only valid to triangular resonator surrounded by a perfect magnetic wall. For a triangular resonator that is not enclosed by a perfect magnetic wall, some modifications need to do. One of the suggestion are by replacing the side length a by an effective value a_{eff} and leaving the substrate dielectric constant unchanged.

$$f_{10} = \frac{2c}{3a_{eff}\sqrt{\epsilon_r}} \quad (2.9)$$

with

$$a_{eff} = a \left[1 + 2.199 \frac{h}{a} - 12.853 \frac{h}{a\sqrt{\epsilon_r}} + 16.436 \frac{h}{a\epsilon_r} + 6.182 \left(\frac{h}{a} \right)^2 - 9.802 \frac{1}{\sqrt{\epsilon_r}} \left(\frac{h}{a} \right)^2 \right] \quad (2.10)$$

the resonance frequency for higher modes can be calculated:

$$f_{mn} = f_{10} \sqrt{m^2 + mn + n^2} \quad (2.11)$$

2.6 Feeding Techniques

Feeding techniques are important in designing the antenna to make sure antenna structure can operate at full power of transmission. Designing the feeding techniques for high frequency, need more difficult process. This is because of input loss on feeding increase depending on frequency, and finally give huge effect on overall design.

There are a few techniques that can be used. Two techniques are used in this project there are coaxial probe feeding and side feed microstrip line.

2.6.1 Coaxial Probe Feed

Figure 2.7 show coaxial probe feeding techniques. This method was the favorite technique for microstrip antenna. Line feeding is connected directed to the radiated metal using a SMA connector from bottom part of substrate. The advantage is the losses on feeding line are too small. This feeding technique is not suitable for high frequency antenna.

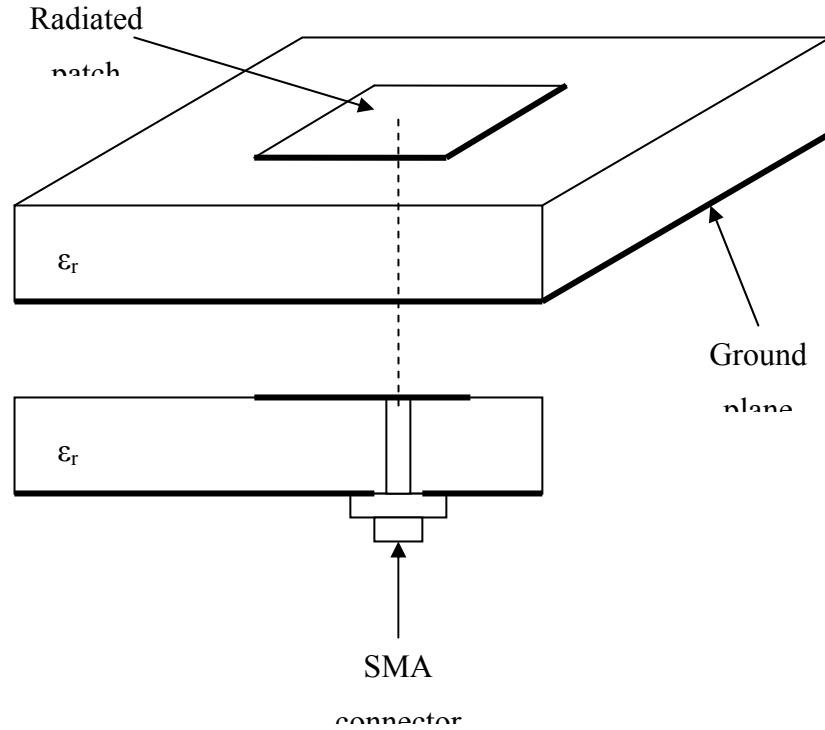


Figure 2.7: Structure antenna with coaxial probe feeding technique.

2.6.2 Side Feed

For side feed technique (Figure 2.8), transmission line feed are connected with radiated patch. Transmission line can be connect to both radiating edge of non-radiating edge side of the antenna. if the feed is move along the antenna side, the input impedance is also changing. In this case, matching impedance must be careful.

The length of feeding line must be in quarter wave length ($\lambda_g/4$) where:

$$\lambda_g = \frac{\lambda_o}{\sqrt{\epsilon_{reff}}}$$

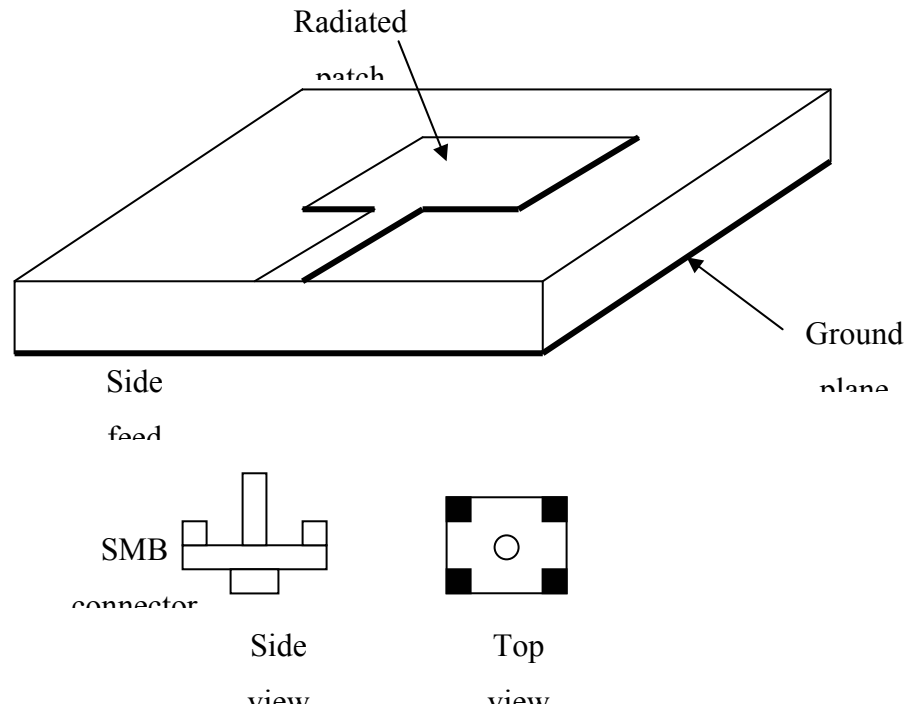


Figure 2.8: Antenna structure with side feed microstrip line.

2.7 Matching Techniques

A system can be considered matched if the VSWR does not exceed 1.5 or mostly 2.0. Once the antenna is well matched there is no power reflected, loss due to dissipation is minimized, the input impedance of the line is independent of frequency

and its length, and problem of dielectric breakdown and excessive heating associated with VSWR is avoided.

There many techniques used for matching. Usually for antenna, quarter wave transformer are prefer and the most easily techniques. Quarter wavelength transformer is used as the side feed. If the impedance of the antenna is real, the transformer is attached directly to the load. If the antenna impedance, Z_L is complex, the transformer is placed a distance d_1 away from the antenna as shown in Figure 2.9. The distance d_1 is chosen to make sure the input impedance towards the load is real. To provide a match, the transformer characteristic impedance Z_o should be [3]:

$$Z_o = \sqrt{Z_L Z_{in}} \quad (2.12)$$

where Z_{in} is the impedance of the input transmission line which is equal to 50Ω .

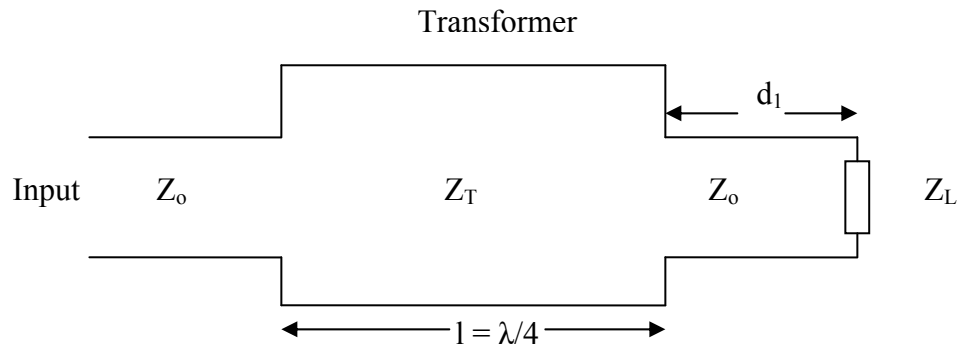


Figure 2.9: Matching with single section quarter wave transformer.

Once Z_o and Z_T are known, to implement into microstrip line, width (w) of the line will play important role to determine the impedance. Transmission line equation can be used to obtain suitable w or just use TXLINE software provides by MICROWAVE OFFICE.

2.8 Summary

In this chapter, the fundamental of antenna theory was cover. Antenna can be described by their characteristic properties. This includes the input impedance, VSWR, gain, radiation pattern, beamwidth, directivity, polarization and bandwidth. Microstrip antennas are popular due to multiple advantages that can be seen to outwear their weakness. In analysis of microstrip antenna main mode of analysis are the transmission line model, cavity model, and full-wave analysis. Accuracy of these methods inverse proportional through their complexity. The transmission line model is less precise, compare to both cavity and full-wave model but exhibit easier implementation. It has been noted cavity model on the other hand present a good trade of between precision and complexity in designing antenna. Through this model design configuration formulation for equilateral triangle, resonance frequency can be derived. In this project, two types of feeding are used that are side feed and coaxial probe feed.

CHAPTER 3

FRACTAL ANTENNA

3.1 Fractal Background

In modern wireless communication systems and increasing of other wireless applications, wider bandwidth, multiband and low profile antennas are in great demand for both commercial and military applications. This has initiated antenna research in various directions, one of them is using fractal shaped antenna elements. Traditionally, each antenna operates at a single or dual frequency bands, where different antenna is needed for different applications.

Fractal shaped antennas have already been proved to have some unique characteristics that are linked to the geometry properties of fractal. Fractals were first defined by Benoit Mandelbrot [14] in 1975 as a way of classifying structures whose dimensions were not whole numbers. Fractal geometry has unique geometrical features occurring in nature. It can be used to describe the branching of tree leaves and plants, rough terrain, jaggedness of coastline, and many more examples in nature. Fractals have

been applied in various field like image compression, analysis of high altitude lightning phenomena, and rapid studies are apply to creating new type of antennas.

Nature does everything to make evolution the most complete balanced system. Fractals are geometric forms that can be found in nature, being obtained after millions of years of evolution, selection and optimization.

The term fractal was first mentioned by French mathematician B.B. Mandelbrot during 1970's after his research on several naturally occurring irregular and fragmented geometries not contained within the realms of conventional Euclidian geometry [14]. These geometries were generally discarded as formless, but Mandelbrot discovered that certain special features can be associated with them.

Mandelbrot defined fractal in several ways. This depends on the definition of their dimension. *A fractal is a set for which the Hausdorff Besicovich dimension strictly exceeds its topological dimension.* Every set having non-integer dimension is a fractal but it can have integer dimension. Fractal is defined by a set of F such that:

- F has a fine structure with details on arbitrarily small scales.
- F is too irregular to be described by traditional geometry.
- F having some form of self similarity
- F can be described in a simple way, recursively
- Dimension of F is greater than its topological dimension.

The dimension of geometry can be defined in several way, some examples are topological dimension, Euclidean dimension, self-similarity dimension, and Hausdorff dimension. The most easily to understand definition is self-similarity dimension. An object is said to be self similar if it looks roughly the same on any scale. The estimated length, L of an object, equal the length of the ruler , r , multiplied by a number, N , of

such rules needed to cover the measure object. For example if there is n copies of original geometry scaled down by a fraction f , the similarity dimension D is defined as :

$$D = \frac{\log N}{\log r} \quad (3.1)$$

D does not need to be integer as in the Euclidean geometry but can be a fraction as in fractal geometry and it is known as the Hausdorff dimension. These have been proven useful in describing natural objects and specifically object that can be used as fractal antennas.



Figure 3.1: A fern is example geometry in nature that is easily modeled using fractal [7].

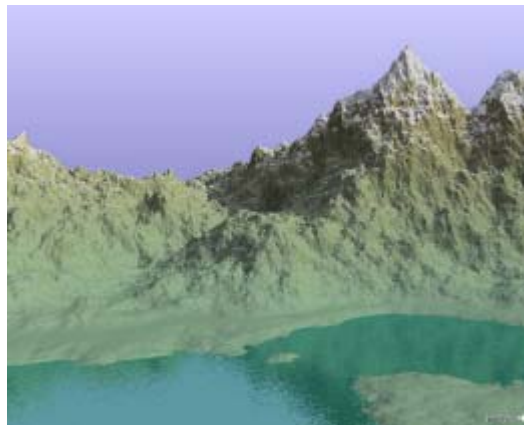


Figure 3.2: Landscape scene that also can be modeled using fractal geometry [28].



Figure 3.3: Fractals are geometric forms that can be found in nature, being obtained after millions of years of evolution, selection and optimization [7].

3.2 Fractal Antennas Elements

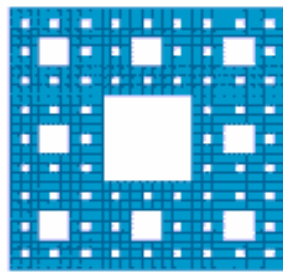
There are many benefits when we applied this nature power (fractals) to develop various antenna elements. By applying fractals to antenna elements:

- We can create smaller antenna size.
- Achieve resonance frequencies that are multiband.
- May be optimized for gain.
- Achieve wideband frequency band.

Most fractals have infinite complexity and detail that can be used to reduce antenna size and develop low profile antennas. For most fractals, self-similarity concept can achieve multiple frequency bands because of different parts of the antenna are similar to each other at different scales. The combination of infinite complexity and detail and self similarity makes it possible to design antennas with very wideband performances.

3.3 Fractal Geometry

There are many fractal geometries that have been found to be useful in developing new and innovative design for antennas. Figure 3.4 shows some of these unique geometries.



Sierpinski carpet



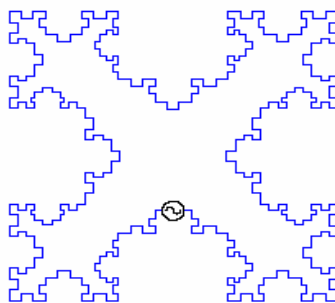
Cantor set



Koch curves



Sierpinski gasket



Koch fractal loop

Figure 3.4: Example of others fractal antennas [8].

3.3.1 Sierpinski Carpet

The Sierpinski carpet is constructed analogously to the Sierpinski gasket, but it uses squares instead of triangles. In order to start this type of fractal antenna, it begins with a square in the plane, and then divides it into nine smaller congruent squares where the open central square is dropped. The remaining eight squares are divided into nine smaller congruent squares which each central are dropped.

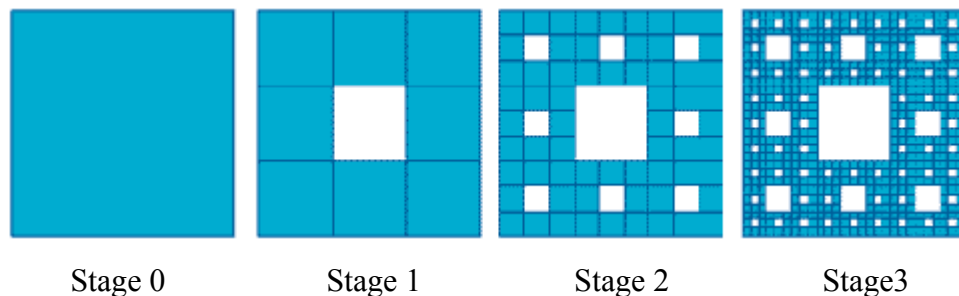


Figure 3.5: Four stages in construction of Sierpinski carpet [8].

3.3.2 Koch Curves

The geometric construction of the standard Koch curve is fairly simple. It starts with a straight line as an initiator. This is partitioned into three equal parts, and the segment at the middle is replaced with two others of the same length. This is the first iterated version of the geometry and is called the generator. The process is reused in the generation of higher iterations.

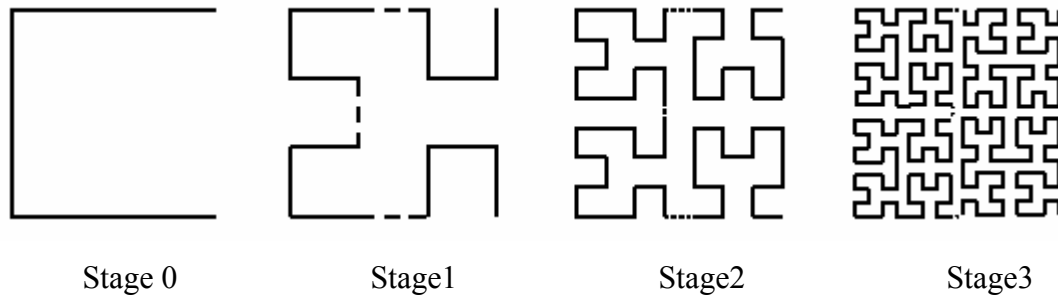


Figure 3.7: Four stage in construction of Hilbert curves [8].

3.4 Sierpinski Gasket Geometry

Sierpinski gasket geometry is the most widely studied fractal geometry for antenna applications. Sierpinski gaskets have been investigated extensively for monopole and dipole antenna configurations [6]. The self-similar current distribution on these antennas is expected to cause its multi-band characteristics [6]. It has been found that by perturbing the geometry the multi-band nature of these antennas can be controlled [18]. Variations of the flare angle of these geometries have also been explored to change the band characteristics of the antenna [17]. Antennas using this geometry have their performance closely linked to conventional bow-tie antennas. However some minor differences can be noticed in their performance characteristics. It has been found that the multi-band nature of the antenna can be transformed into wideband characteristics by using a very high dielectric constant substrate and suitable absorbing materials.

3.4.1 Generation of Sierpinski Gasket Fractal Geometry

The generation of Sierpinski gasket geometry is explained using Figure 3.8. Although the geometry presented here consists of equilateral triangles, the description here holds good for any triangular geometry. Explanations of its generation are in two ways:

- The multiple copy approach
- Decomposition approach

For the first, one starts with a small triangle. Two more copies of this triangle (same size) are generated and attached to the original triangle. This process can be done n number of times, n being the order of the fractal iteration. In the decomposition approach, one starts with a large triangle encompassing the entire geometry. The midpoints of the sides are joined together, and a hollow space in the middle is created. This process divides the original triangle to three scaled down (half sized) versions of the larger triangle. The same division process can be done on each of the copies. After n such divisions, the geometry shown in the figure is obtained. Affine transformations, of which similarity transformations form a convenient sub-class, are important characteristics of fractal geometries. These involve scaling, rotation and translation. These transformations can be expressed in the mathematical form as:

$$W \begin{pmatrix} x \\ y \end{pmatrix} = \begin{bmatrix} r \cos \theta & -s \cos \phi \\ r \sin \theta & s \sin \phi \end{bmatrix} \begin{pmatrix} x \\ y \end{pmatrix} + \begin{pmatrix} x_0 \\ y_0 \end{pmatrix} \quad (3.1)$$

r and s are scale factors

θ and ϕ correspond to rotation angles

x_0 and y_0 are translations involved in the transformation

If r and s are both reductions ($r, s < 1$) or both magnifications ($r, s > 1$), the transformation is *self-affine*. If $r = s$ and $\theta = \varphi$, the transformation is *self-similar*. First the generation of ‘strictly self-similar’ Sierpinski gasket is considered. Starting with an equilateral triangle of unit length side the transformations involved to get the next iterated geometry.

Multiple Copy Approach

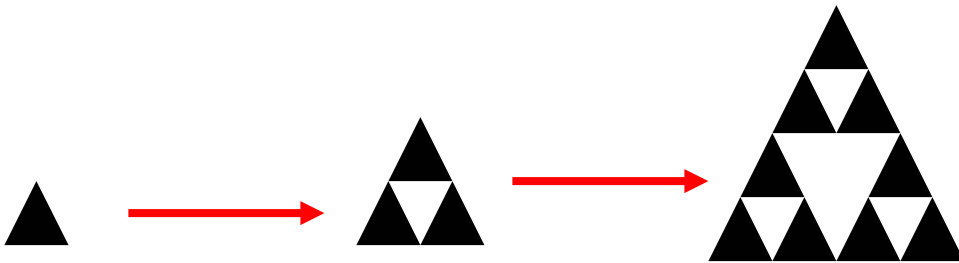


Figure 3.8: Multiple copy generation approach.

Decomposition Approach

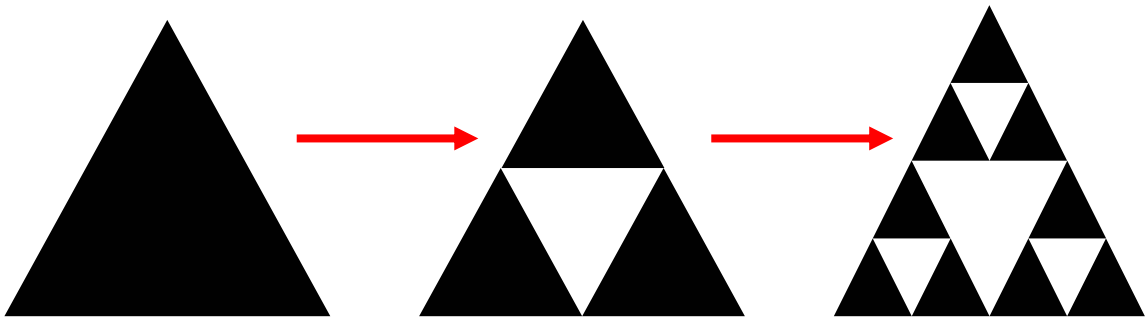


Figure 3.9: Decomposition generation approach.

It is assumed that the origin of the co-ordinate system is at the bottom left corner of the triangle, and the x -axis pass through the base (bottom) side of the triangle. The transformations W_1 , W_2 , W_3 are indicated in Fig. (4.9). The second geometry is obtained with a union of these three transformations:

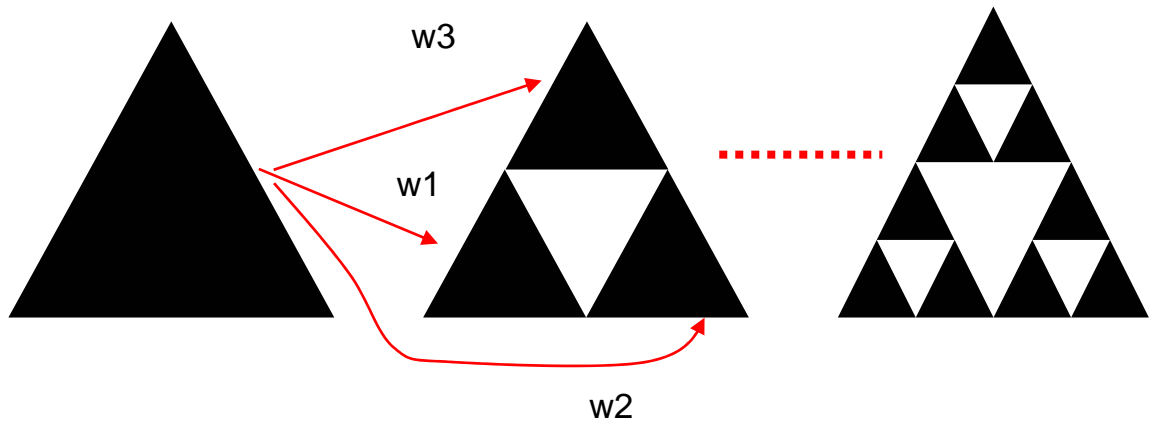


Figure 3.10: Iterated Function System (IFS) for generation of self-similar Sierpinski gasket geometry.

$$W1 \begin{pmatrix} x \\ y \end{pmatrix} = \begin{bmatrix} 0.5 & 0 \\ 0 & 0.5 \end{bmatrix} \begin{pmatrix} x \\ y \end{pmatrix}$$

$$W2 \begin{pmatrix} x \\ y \end{pmatrix} = \begin{bmatrix} 0.5 & 0 \\ 0 & 0.5 \end{bmatrix} \begin{pmatrix} x \\ y \end{pmatrix} + \begin{pmatrix} 0.5 \\ 0 \end{pmatrix}$$

$$W3 \begin{pmatrix} x \\ y \end{pmatrix} = \begin{bmatrix} 0.5 & 0 \\ 0 & 0.5 \end{bmatrix} \begin{pmatrix} x \\ y \end{pmatrix} + \begin{pmatrix} 0.25 \\ 0.433 \end{pmatrix}$$

$$W(A) = W1(A) \cup W2(A) \cup W3(A)$$

This process of generation of the geometry is very convenient in the context of computer platforms, and is often called *multiple reduction copy machine* (MRCM). In mathematics, these are referred to as *iterated function systems* (IFS).

3.5 Sierpinski Gasket Monopole

Most antenna designs are highly frequency dependent where the size of the antenna relative to the operating wavelength. Carles Puente [10] first describe the multiband behavior of Sierpinski gasket monopole geometry. Such behavior is based on the self-similarity properties of the antenna's fractal shape, which open alternative way for designing new multiband and frequency independent antennas (FIA).

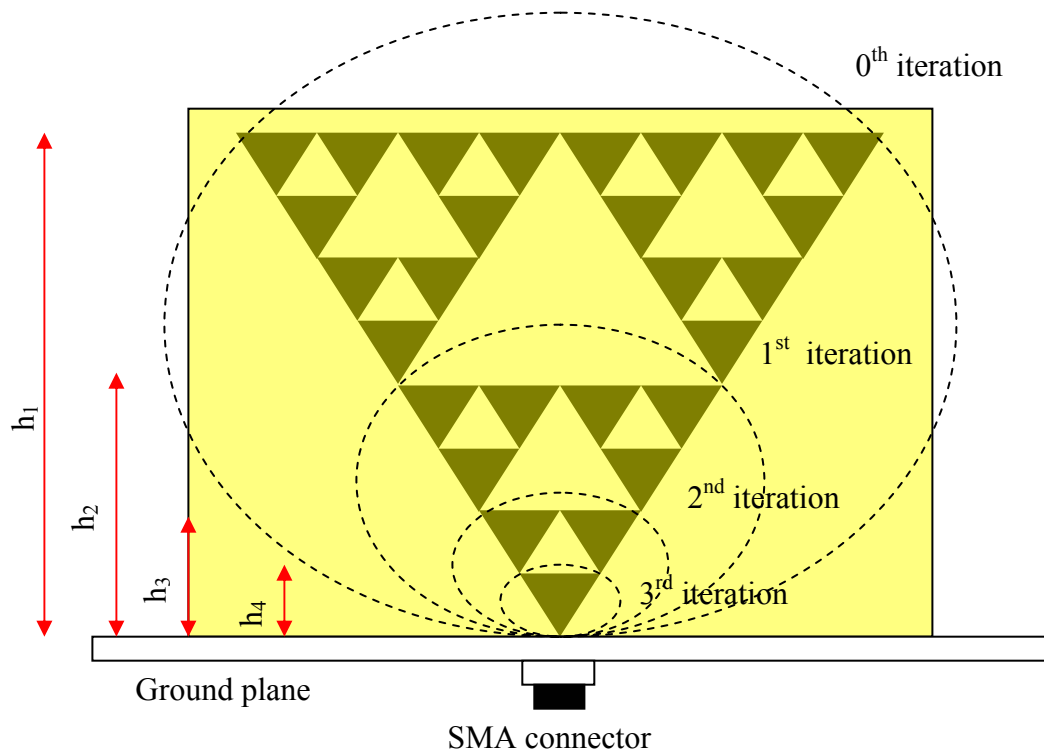


Figure 3.11: Sierpinski gasket monopole antenna.

The scale factor will determine the high of each sub gasket and given by:

$$\delta = \frac{h_n}{h_{n+1}} \quad (3.2)$$

Figure 3.11 show a third iteration of the fractal Sierpinski gasket. The high of each sub-gasket will determined of resonant frequency of antenna. This means we will get 4 different bands because of 4 different high of sub-gasket. By changing the scale factor we will get different high of each sub-gasket, therefore different frequency band.

From [12] , to determine the monopole Sierpinski gasket antenna, the simplified equation is given by:

$$fr = k \frac{c}{h} \cos(\alpha / 2)(\delta)^n \quad (3.3)$$

where

c	speed of light
h	height of monopole
α	flare angle
δ	scale factor
n	band number
k	0.152

Flare angle is the angle of the inside of the triangle. In this project the flare angle was chosen to be 60° as a starting point. The constant k as given in [12] as 0.15, is depend on the dielectric substrate type and thickness used. It is only use as a first guess for this project and final parameters are fully confirmed through simulation.

3.6 Design Procedure.

In this project, the substrates material that is used is FR4 board. Several reasons why this type is chosen because of it is among the cheapest board in market. The FR4 also can operate until 10 GHz frequency. The thickness of the dielectric available is 1.6 mm and loss tangent 0.019. The dielectric substrate FR4 is acceptable for the purpose of proof-of-concept design. Table 3.1 shows the specification of FR4 laminates.

Table 3.1: Laminates specification

Relative dielectric constant	≈ 4.7
Loss tangen δ	0.019
Substrate thickness	1.6 mm
Acceptable frequency range	< 10 GHz

The flow chart of the design procedure is shown in Figure 3.12. For Sierpinski gasket patch, the designs start with an equilateral triangle at 1.8GHz (for SGFpe1, SGFpd1, and SGFm1). Actually for the first 3 antennas, the same dimension is used but different point of feeding. The next step is to choose the relevant material such as the microwave laminate. In this project, the laminate that is chosen is FR4 laminate. After that, the antenna is fractal from 1st to 3rd iteration. Except for SGFm2, the antenna is specifically design at dual band that are 2.4GHz and 5.0GHz.

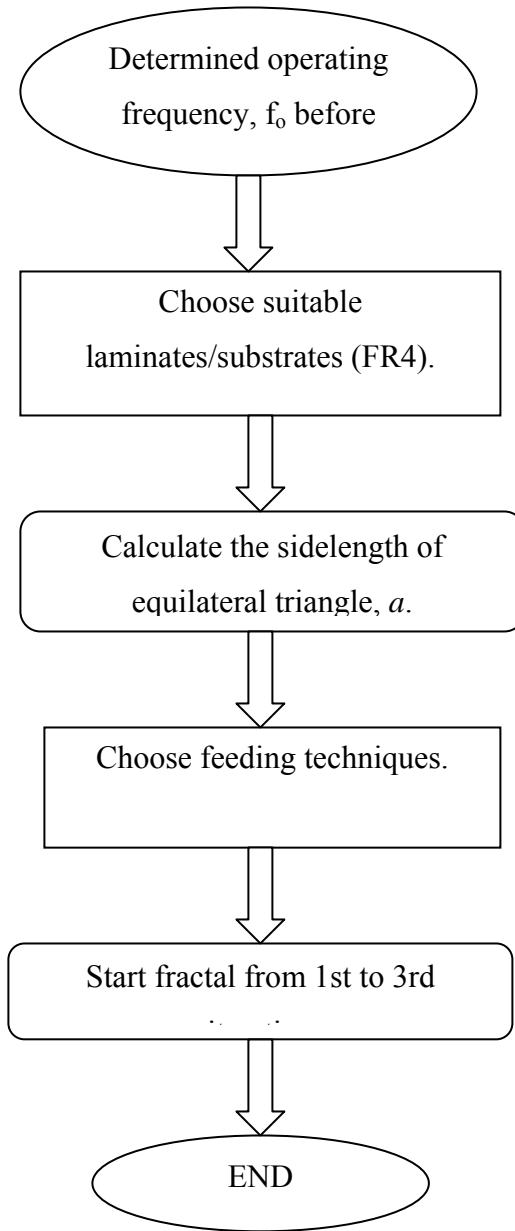


Figure 3.12: Flow chart of the design procedure for SGFpe1, SGFpd1, and SGFm1.

Using previous equation as mentioned in chapter 2, the side length a and height h of equilateral triangle are calculated. In this project as mentioned in previous chapter, the

scale factor chosen is 2, so each fractal the height h of the equilateral triangle need to divide by 2. Table 6.1 shows the dimension of each antenna.

Table 3.2: Dimension for the antennas.

Antenna	SGFpe1	SGFpd1	SGFm1
Side length (mm) a	52	52	52
Height (mm) h	45.03	45.03	45.03

3.6.1 Sierpinski Gasket Patch.

An equilateral triangle patch antenna may be designed by following procedure which assumes that the specified information includes the dielectric constant of the substrate, operating frequency, height of the substrates.

- Specify: ϵ_r, f_0 (1.8 GHz), h
- Side length of equilateral triangle a , is determined (depend on f_0)
- Determine the feeding location.
- Start fractal it from 1st to 3rd iteration. Scale factor $\delta=2$, flare angle= 60° .

Two antennas were designed. There are SGFpe1 and SGFpd1. The step to construct Sierpinski gasket are shown on Figure 3.13.

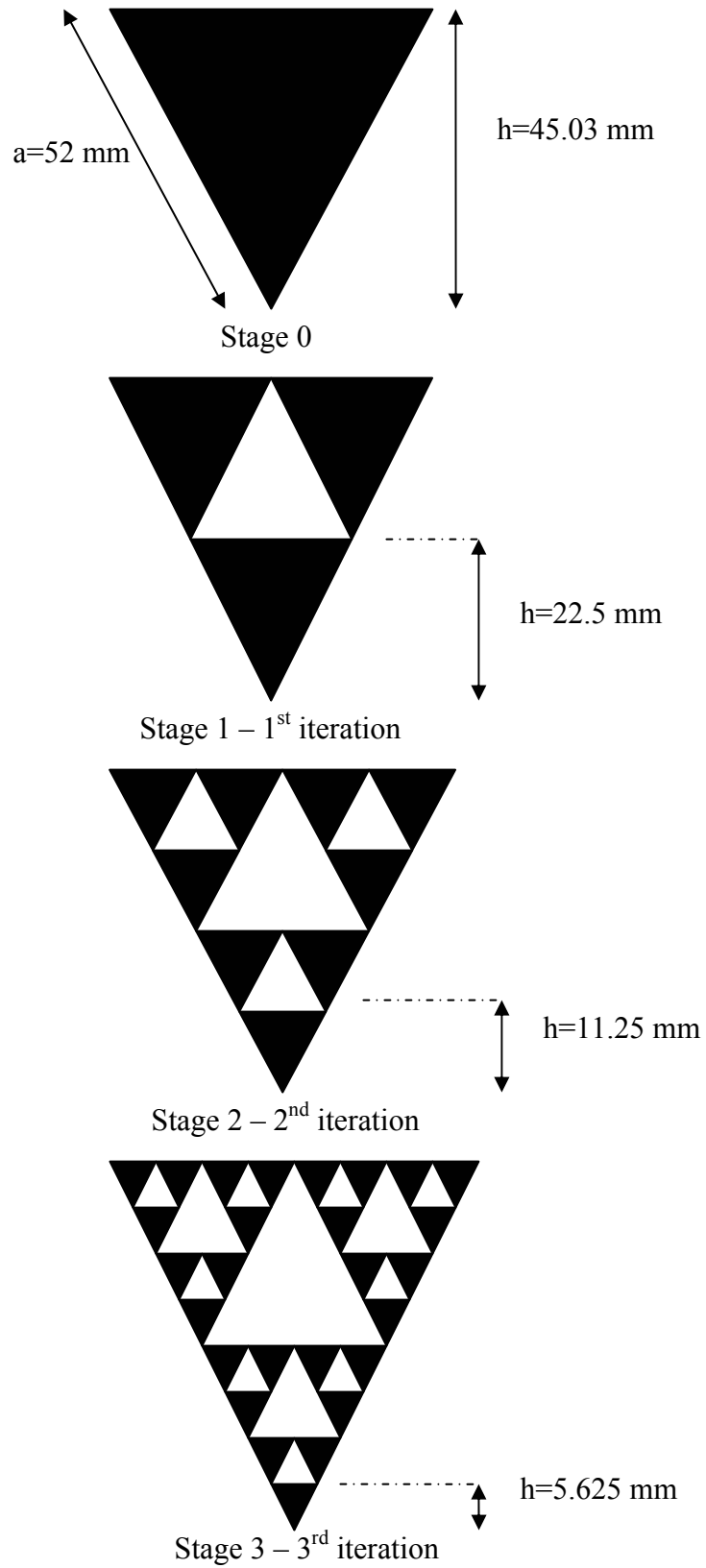


Figure 3.13: Stage of construct Sierpinski gasket patch

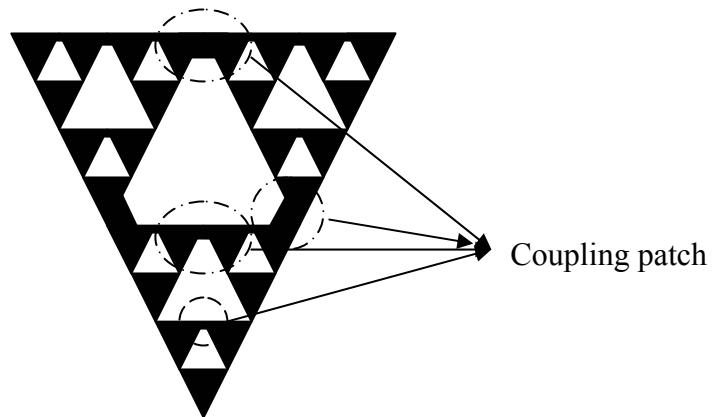


Figure 3.14: Introducing coupling patches-SGFpe1 and SGFpd1.

When higher iteration is done to Sierpinski gasket patch antenna, the structure doesn't radiate effectively. To overcome this problem as suggest by [19], coupling patches are introduced between two isolated triangles to provide low resistance conducting path to the current that attempts to penetrate into upper portion of the structure. The size of coupling patch depends upon triangles that are connected.

3.6.2 Sierpinski Gasket Monopole

SGFm2 is designed at 2.4 GHz and 5.0 GHz. Scale factor need to calculate from the ratio of the resonant frequencies desired: $f_2=2.4$ GHz (second band that required) and $f_3=5.0$ GHz (third band that required).

$$5.0 \text{ GHz}/2.4 \text{ GHz} = 2.08$$

Here, the scale factor= $2.08 \approx 2$. So each triangle structure of the gasket is twice as large as its sub-structure. The height of the triangular structure resonating at f_2 is $h_2=3.1$ cm, the height of the monopole is calculated to be $h=2 \cdot h_2=6.2$ cm. The number of iterations from equation 4.10 needed to generate is $n_{\max}=4$. This means the iteration that will be done until 3 rd iteration. So there are four bands of frequencies, where f_1 and f_4 are included to provide continuity so that truncation effects do not affect the resonant bands of interest (f_2 and f_3). As mentioned in [6] the first resonant bands f_1 , is not in scale of two.

Table 3.3: SGFm2 geometry parameters.

Geometry Parameter	Value
Scale factor, δ	2
Height, h	6.2cm
Flare angle, α	60°
Max iteration, n_{\max}	4

For SGFm1 the dimension is taken from SGFpe1 and feed it like monopole type. This is done to SGFm1 just to observe the behavior of resonant frequencies bands.

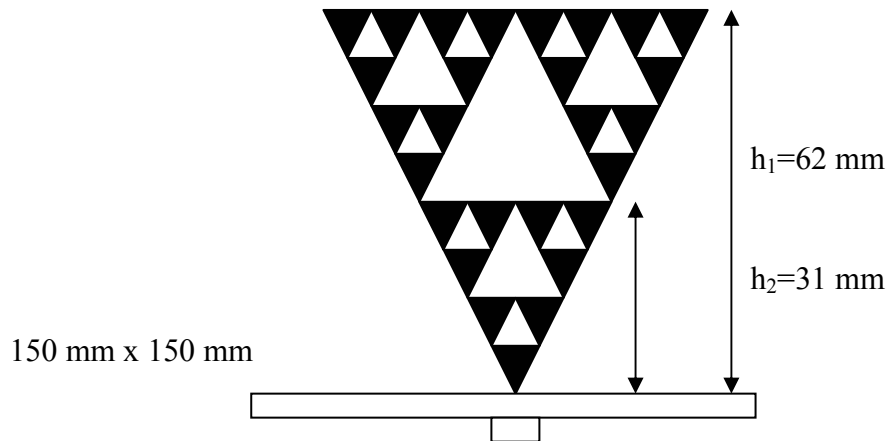


Figure 3.15: Dimension of SGFm2.

3.7 Summary

The concept of fractal can be seen occurring in nature. It is defined as a set for which the Hausdorff Besicovich dimension strictly exceeds its topological dimension. Furthermore the dimension of geometries can be defined through Euclidean dimension, self-similarity dimension, and Hausdorff dimension. Through implementation of these natural phenomena in antenna design, a new class of antenna term as fractal antenna can be designed to achieve smaller, multiple resonant frequencies without degrading the antenna properties. Among the fractal antenna geometries found are Sierpinski carpet, Cantor set, Koch curves, Koch fractal loop and Hilbert curves. The Sierpinski gasket geometry in particular, can be described as multiple iteration of equilateral antenna depend on its scale factor. This chapter has shown in detail design methodology utilized in order to construct both monopole and patch Sierpinski gasket.

CHAPTER 4

SIMULATION, FABRICATION AND MEASUREMENT

4.1 Introduction

The simulation software used in this thesis are Microwave Office and ADS. Microwave Office was used to simulate the designs of Sierpinski gasket microstrip antenna. This software can be design using circuit analysis or EM structure using MoM. For this projects the, the layout are design at the EM structure part. This software also provide TXLINE (Figure4.2) that automatically calculate the length and width of microstrip line for a given certain impedance and frequency operate.

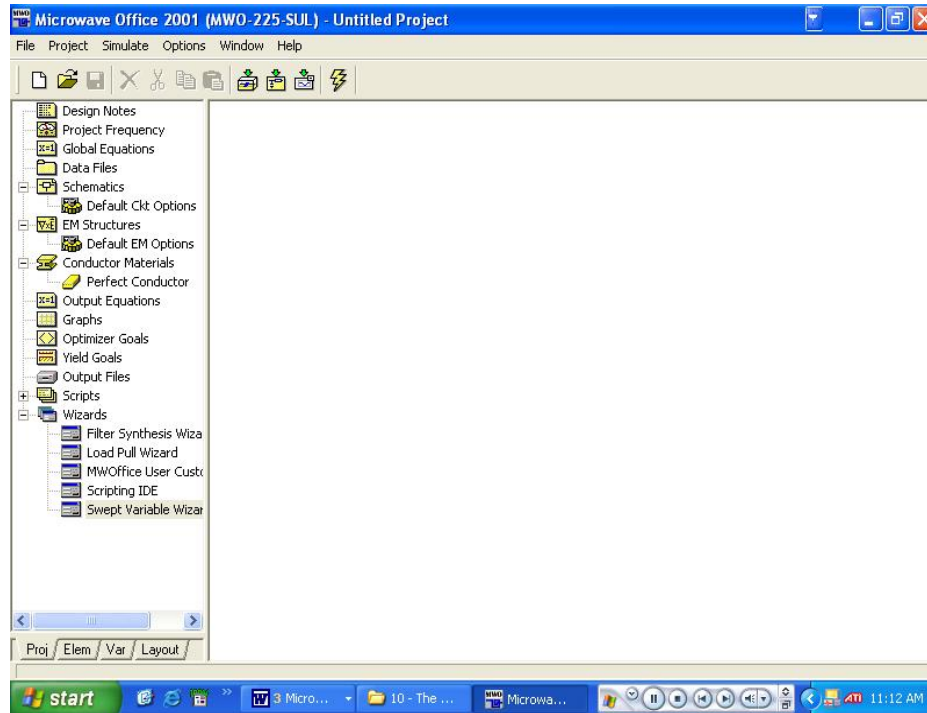


Figure 4.1: Microwave Office Environment

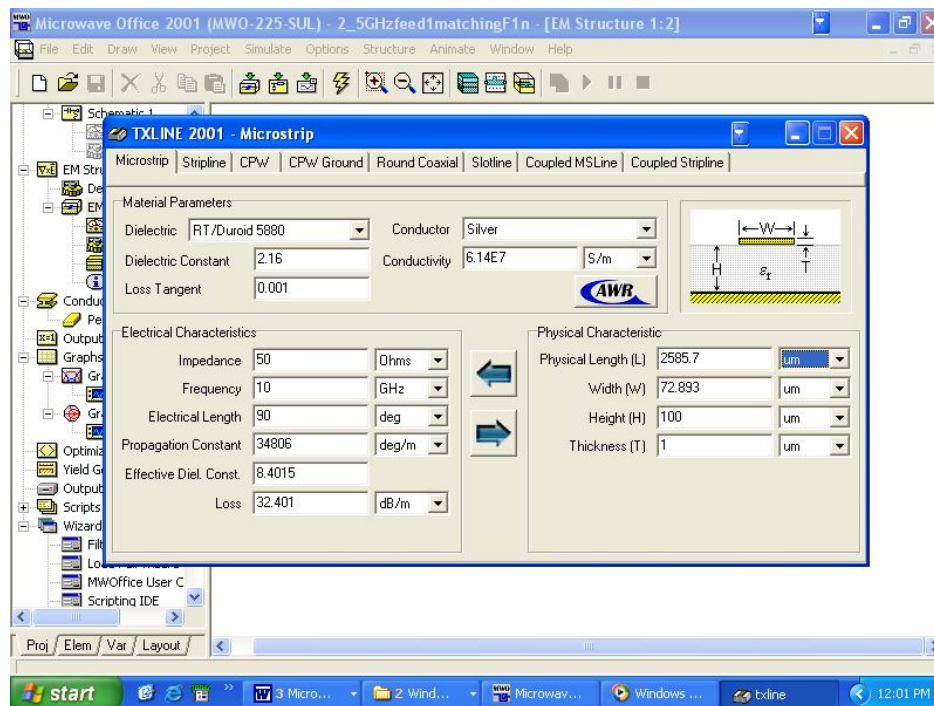


Figure 4.2: TXLINE calculator

The design can be start by right click on EM structure and select New EM structure. Then set the layout dimension on Enclosure menu. The unit must be sure in mm. It is advice to set the optimum dimension of box size at least $\lambda_g/4$ form layout dimension. In the Dielectric Layer menu, key in the parameters of thickness of the substrate, dielectric constant and loss tangent, where their values are 1.6mm, 4.7 and 0.019 respectively.

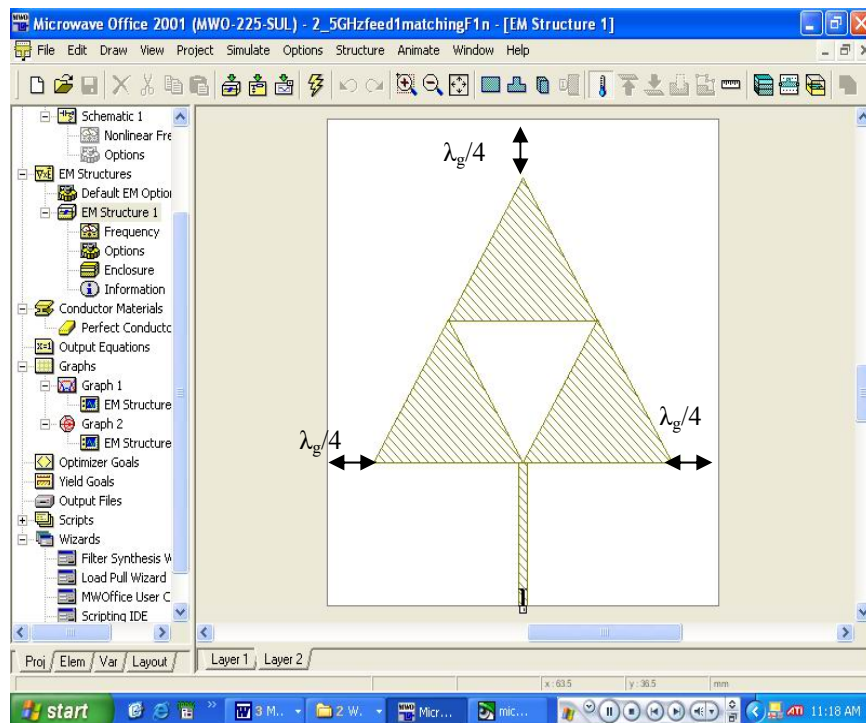


Figure 4.3: Layout design on EM structure

Unpick the “use project frequency”. Set the operation frequency. The observation frequency need to key in is 0 GHz to 10 GHz, while the step of frequency 0.01. In the Boundaries menu, tick the “Approximate open (37 ohms)” for Enclosure Top and “Perfect conductor” for Enclosure Bottom. The layout can be view in 3D to get clear dimension of each layer as shown in Figure 4.4.

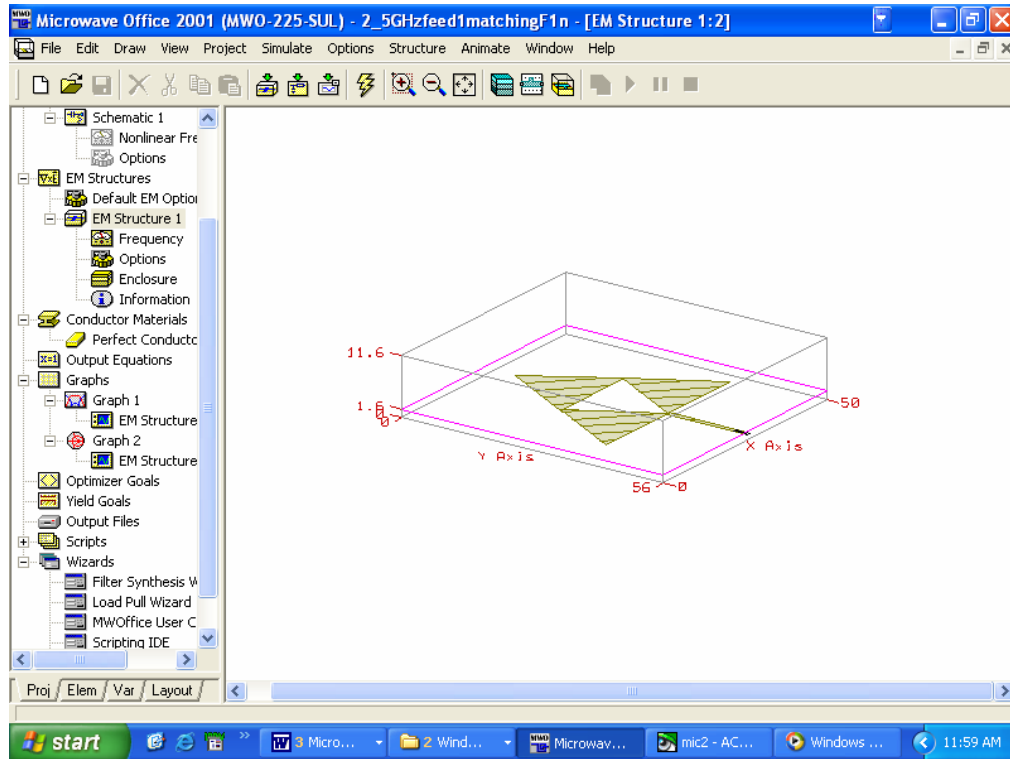


Figure 4.4: 3D view of layout design

It is needed to analyze the simulation results in the format of graphs. Therefore, right click at the Graphs menu and choose Add Graph. After each graph is added, right click at that particular graph menu and choose Add Measurement. Then, the selected measurement type can be chosen. Here the relevant measurements are return loss $[S_{11}]$ in rectangular graph, antenna radiation pattern in polar plot.

4.2 Fabrication

The practical implementation is carried out when the simulation process ends. This involves the artwork preparation for the antenna fabrication as well as etching process and connecting the suitable connector. The layout design in Microwave Office, need to transfer into *.GDS format. Then the *.GDS format need to open at AutoCAD software. Knowledge on the use of AutoCAD is needed here. The reason why using AutoCAD is the layout need to print to transparency in actual size.

4.2.1 Etching Process

Etching process generally consists of four main steps. Microstrip laminates are cut into the required size. Then the plastic layer that covers the film is takeout and put together with the layout design on transparency. Ultraviolet light is then illuminated onto the surface. After 40 seconds, the laminate is immersed into germanium silicate to get layout design onto plate. Then the laminates need to immerse into acid bath. After a few hours, the unwanted metal on laminate will be etched away.

4.2.2 Connecting to Connector.

SMA and SMB connectors are used as the connector to the antenna as a completion of the fabrication process. SMA is connected to monopole fractal antennas, while SMB is connected to microstrip fractal antennas.

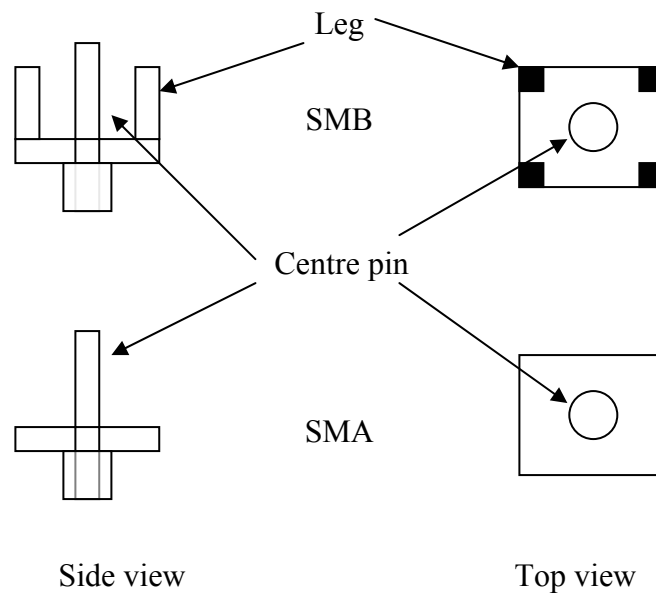


Figure 4.5: Two types of connector that are used.

Figure 4.6 shows the overall process for fabrication from the beginning.

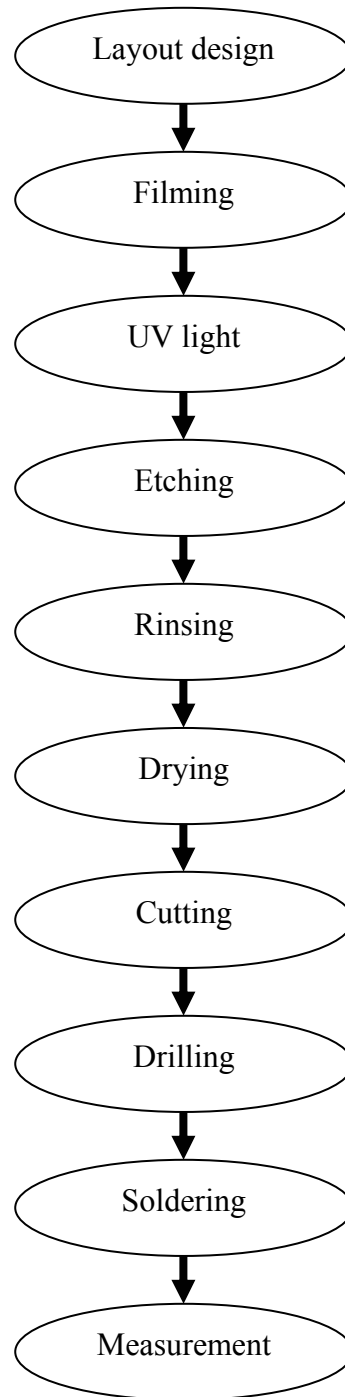
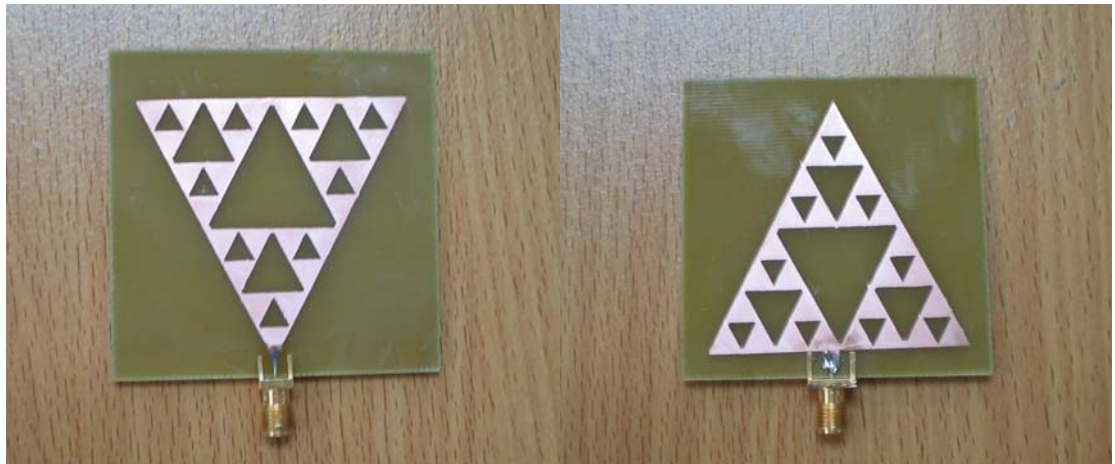


Figure 4.6: Step of fabrication process from beginning to measurement.



SGFpe1

SGFpd1

Figure 4.7: Sierpinski gasket patch antenna.



SGFm1

SGFm2

Figure 4.8: Sierpinski gasket monopole antenna.

4.3 Antenna Measurement.

Antenna characteristics are measured using the network analyzer. It is very convenient and easy to obtain antenna input characteristics using a network analyzer. The return loss (S_{11}) measurement can be obtained from this equipment using single port calibration. The radiation characteristics of antennas can be measured in an anechoic chamber using a spectrum analyzer. The experimental set up is shown in Fig. 4.9. The distance between transmitting and receiving antennas is approximately 3 meters, a signal generator is connected to a horn antenna with 20 dBm gain. This signal generator can be used depending on the frequency of interest. A positioner controller will control the rotation of receiving antenna depend on time setting (every 5 second for this measurement). When a standard antenna (horn) is used as the transmitter and test antenna as the receiver, S_{21} reading is written down manually. First the horn must be in horizontal facing the vertical receiver antenna to get the E co-polar of the receiver antenna. Next the horn is in vertical without changing the receiver antenna and the readings of E cross-polar are taken. Then the receiver antenna have to turn to horizontal side with the horn in horizontal and vertical side to get H co-polar and H-cross-polar.

A comparison method is adopted for antenna gain measurements. This assumes the return loss of the test antenna is very small and comparable with that of a standard antenna. Here we need two standard (horn) antennas. First the horn antenna is placed on the positioner, aligned with the transmitter (another horn). S_{21} is measured using the network analyzer. The network analyzer may be normalized with this measurement data. Next the standard antenna at the receiver is replaced with the test antenna without disturbing the rest of the set up. The test antenna is aligned at the direction of its peak by controlling the positioner. S_{21} is measured for the test antenna. The difference in these S_{21} measurements is added to the known gain of the standard antenna to obtain the gain of the test antenna.

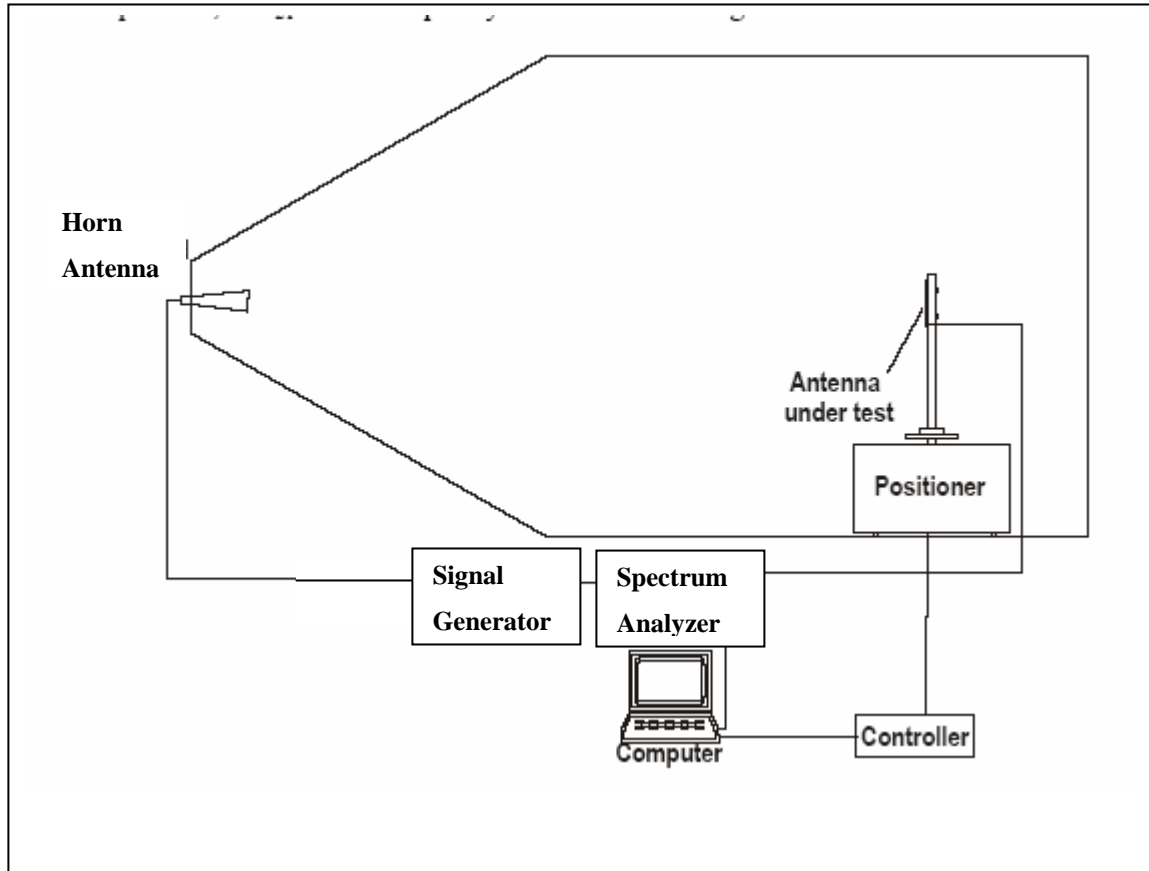


Figure 4.9: Radiation pattern measurement setup.

4.4 Summary

The important parameter analysis of simulation software has been discussed in this chapter. This chapter has shown in detail the fabrication process and a measurement setup also has been explained here.

CHAPTER 5

RESULTS AND DISCUSSION

5.1 Introduction

Four antennas have been fabricated and tested. Simulation and measurement results are discussed and compare in this chapter.

5.2 Simulation Results

(a) SGFpe1

The design starts at 1.8 GHz, when one edge of the antenna is direct feed to SMB connector the return loss result are not good. The reason why the feed direct to one of edge is because of we want the wave propagate follow the dimension of the antenna shape. The 1st iteration is shown in Figure 5.1, there exist one band frequency around

6.5 GHz and return loss is quite good at -18.088 dB. Bandwidth in percentage for 6.5 GHz is around 2.4.

Table 5.1: Frequency band, return loss and bandwidth.

Band	f (GHz)	S ₁₁ (dB)	BW	f _n /f _{n+1}
m ₁	6.531	-18.088	2.4	-

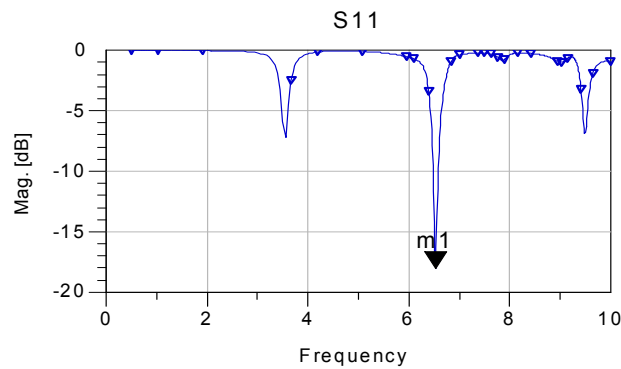


Figure 5.1: Return loss response of SGFpe1 at 1st iteration.

Then, for the same antenna, SGFpe1 is fractal again for at 2nd iteration. The results are shown in Table 5.2 and Figure 5.2. Only one frequency band exist at 6.9 GHz but return loss response only reach -10.69dB.

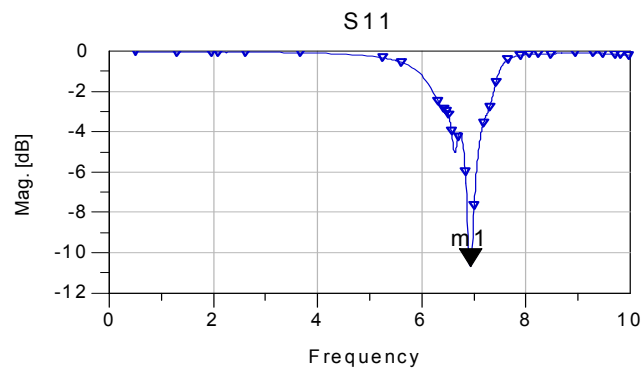


Figure 5.2: Return loss response of SGFpe1 at 2nd iteration

Table 5.2: Frequency band, return loss and bandwidth

Band	f (GHz)	S ₁₁ (dB)	BW	f _n /f _{n+1}
m ₁	6.932	-10.679	0.8	-

When SGFpe1 is fractal to 3rd iteration four frequency bands exist at higher frequency. There one frequency band exist at low frequency but thee return loss is not good enough. Return loss for the three bands at higher frequency are in good condition. All the bandwidth of each band are in narrowband category.

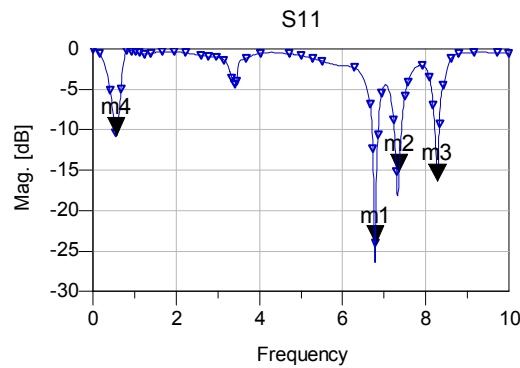


Figure 5.3: Return loss response of SGFpe1 at 3rd iteration

Table 5.3: Frequency band, return loss and bandwidth

Band	f (GHz)	S ₁₁ (dB)	BW	f _n /f _{n+1}
m ₁	0.556	-10.648		-
m ₂	6.790	-24.007	2.24	12.05
m ₃	7.361	-15.182	3.12	1.08
m ₄	8.281	-16.352	1.57	1.12

(b) SGFpd1

This type of antenna is direct transmission line feed at point nearly 50Ω impedance. When this antenna is fractal at first iteration the result are shown in Figure 5.4 and Table 5.4. Two frequency bands exist at 6.39 GHz and 9.86 GHz. Both of them have good return loss and the ratio between both frequencies is 1.54. The input impedance for the first band is 50.894Ω and for the second band around nearly 52Ω , respectively.

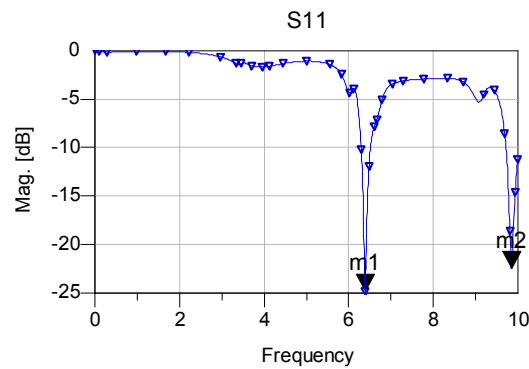


Figure 5.4: Return loss response of SGFpd1 at 1st iteration

Table 5.4: Frequency band, return loss and bandwidth

Band	f (GHz)	S_{11} (dB)	BW	f_n/f_{n+1}
m ₁	6.389	-24.877	6.15	-
m ₂	9.861	-22.51	6	1.54

For second iteration, there are three bands exist for the observation. The gap between first and second band are quite close at 3.2 GHz and 3.59 GHz. The last frequency band quite a wide bandwidth around 1GHz cover from 7 to 8 GHz. All the impedance for the first, second, and third bands are nearly 50Ω which are 49.987Ω , 50.08Ω , and 51.2Ω .

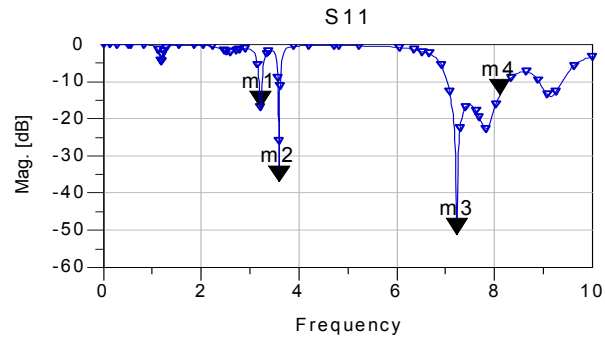


Figure 5.5: Return loss response of SGFpd1 at 2nd iteration

Table 5.5: Frequency band, return loss and bandwidth

Band	f (GHz)	S_{11}	BW	f_n/f_{n+1}
m ₁	3.210	-16.912	2.65	-
m ₂	3.591	-37.504	1.42	1.12
m ₃	7.229	-51.205	17.1	2.01

When the last iteration done to SGFpd1, it doesn't give good return loss. All of S_{11} reading doesn't reach below than -10dB. According to [19], the structure doesn't radiate effectively. The solution for this problem is by introduced the coupling patches between two isolated triangles, with a view to provide low resistance conducting path to the currents that attempts to penetrate into the upper portion of the structure. The size of the coupling patch depends upon the triangles that are to be connected. For the modified geometry, new resonance frequencies appear at 6.952 GHz, 7.524 GHz, and 8.596 GHz. Actually there are other low frequencies appear at 1 GHz, 3.5 GHz, and 4 GHz but all doesn't reach below -10dB for return loss. All the resonance frequency are in narrowband. These three frequencies band impedance value are at 51.12Ω , 51.3Ω , and 51.88Ω .

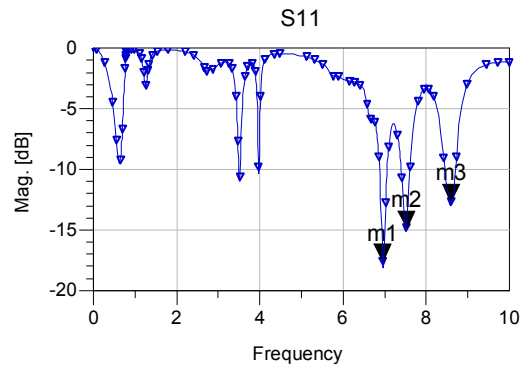


Figure 5.6: Return loss response of SGFpd1 at 3rd iteration

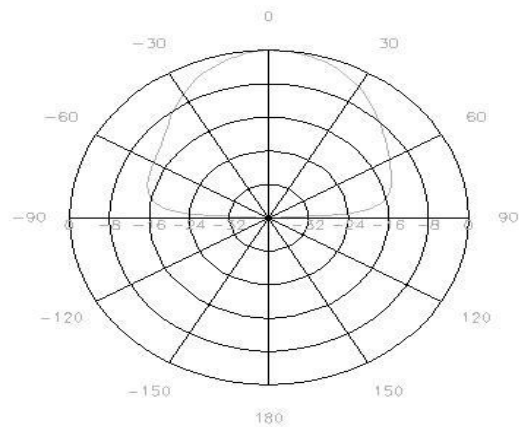
Table 5.6: Frequency band, return loss and bandwidth

Band	f (GHz)	S ₁₁ (dB)	BW	f _n /f _{n+1}
m ₁	6.952	-17.629	3.35	-
m ₂	7.524	-14.853	2.68	1.08
m ₃	8.596	-12.690	3.57	1.14

Due to software constrain, all Sierpinski Gasket monopole type cannot be simulate. So the results of SGFm1 and SGFm2 only get from experiment.

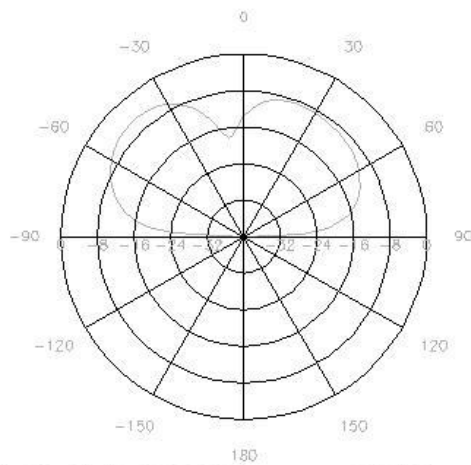
(c) Radiation Pattern

Figure 5.7-5.10 shows the radiation pattern for SGFpe1 and SGFpd1 at 3rd iteration. The radiation pattern are cut at the E plane ($\varphi=0^\circ$) and H-plane ($\varphi=90^\circ$). Both antenna radiation patterns show slight dip near 90° for second resonance frequency.

$f_1=6.79$ GHz

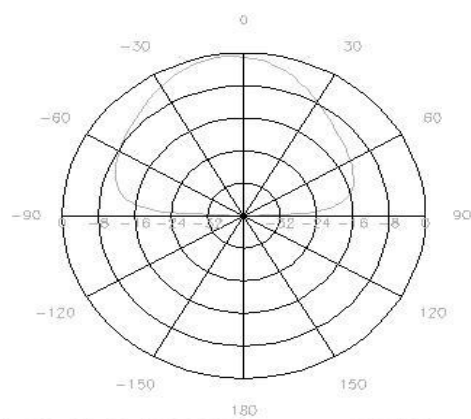
Mon Feb 25 01:14:25 2002

EF318c

 $f_2=7.36$ GHz

Mon Feb 25 01:18:02 2002

EF318c

 $f_3=8.28$ GHz

Mon Feb 25 01:02:46 2002

EF318c

Figure 5.7: Radiation pattern simulation at $\Phi=0$ cut (E-plane) for SGFpe1.

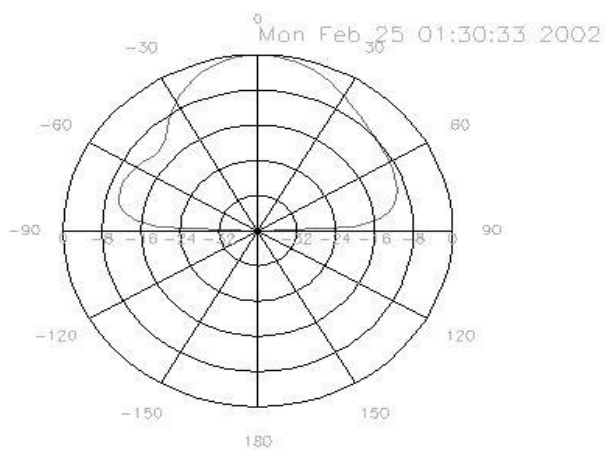
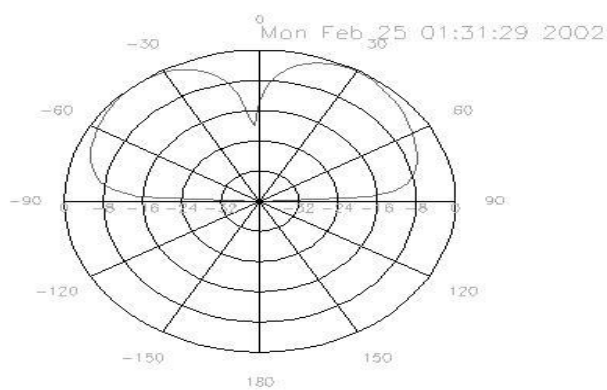
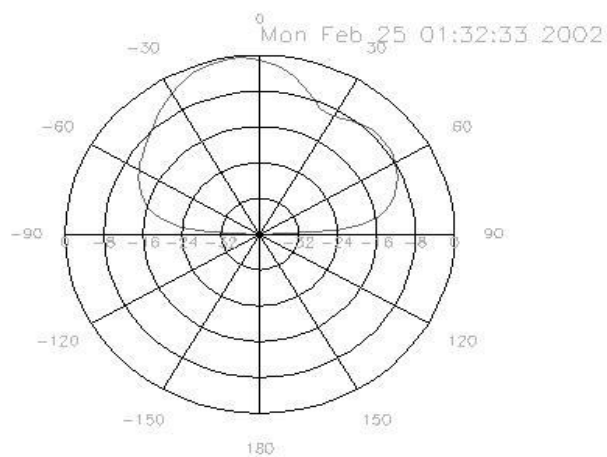
$f_1=6.79$ GHz $f_2=7.36$ GHz $f_3=8.28$ GHz

Figure 5.8: Radiation pattern simulation at $\Phi=90$ cut (H-plane) for SGFpe1.

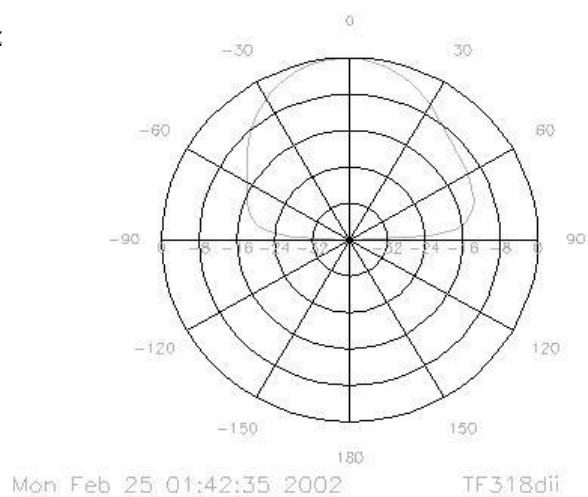
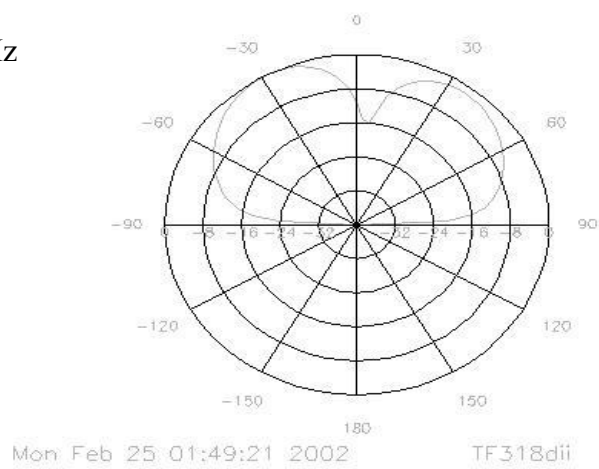
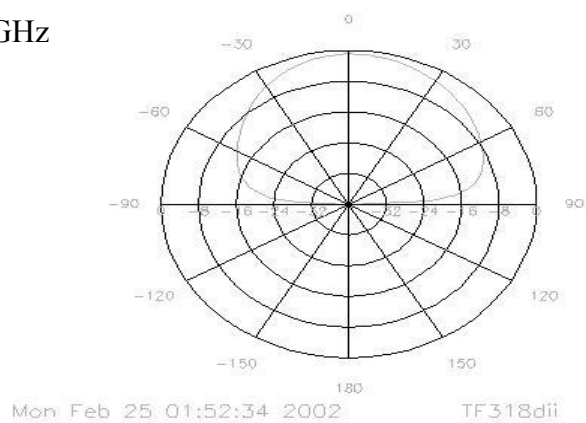
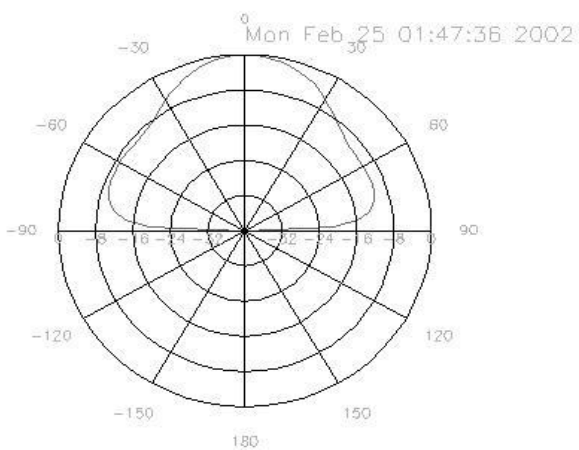
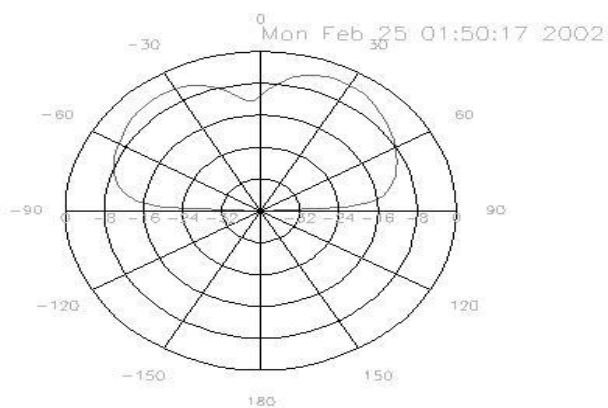
$f_1=6.95$ GHz $f_2=7.52$ GHz $f_3=8.596$ GHz

Figure 5.9: Radiation pattern simulation at $\Phi=0$ (E-plane) for SGFpd1.

$f_1=6.95$ GHz



$f_2=7.524$ GHz



$f_3=8.28$ GHz

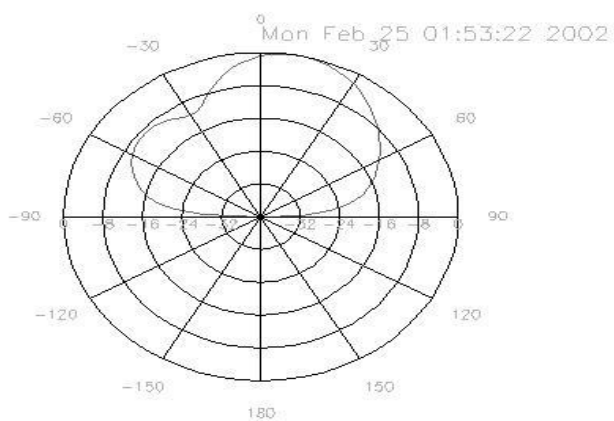


Figure 5.10: Radiation pattern simulation at $\Phi=90$ (H-plane) for SGFpd1.

5.3 Measurements Result

Antennas SGFpe1, SGFpd1, SGFm1, and SGFm2 at 3rd iteration are fabricated and tested. The simulation and measurement for return loss are compared.

(a) SGFpe1

Figure 5.11 show the comparison between simulation and measurement result. At the beginning the S_{11} response are quite similar for both simulation and actual measurement. Both graph show the frequency band concentrate at higher frequency.

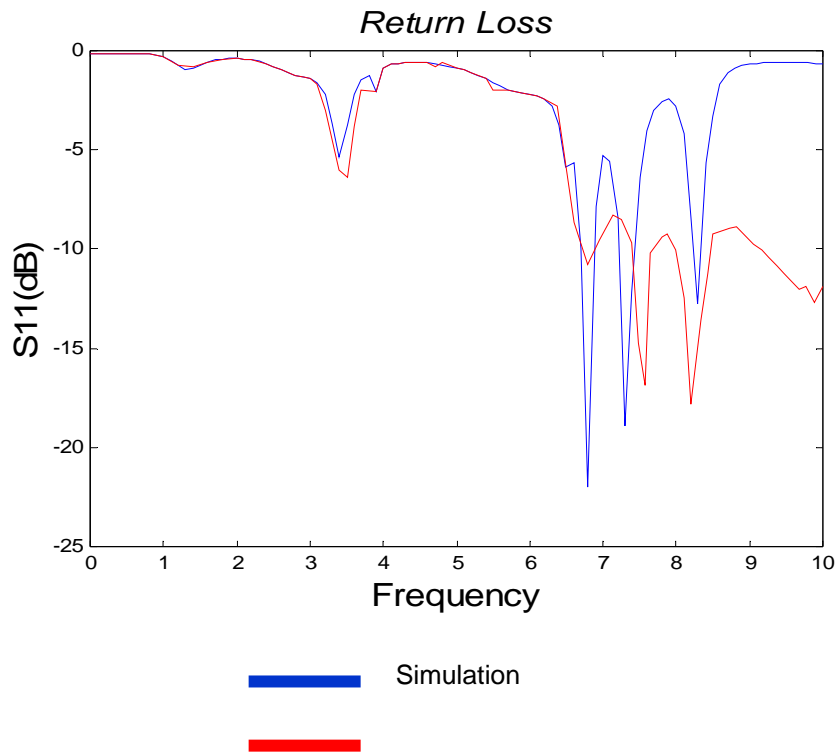


Figure 5.11: Comparison simulation and measurement of SGFpd1 antenna.

Table 5.7: Frequency band, return loss and bandwidth for measurement

Band	f (GHz)	S ₁₁ (dB)	BW	f _n /f _{n+1}
m ₁	7.57	-16.88	3.26	-
m ₂	8.2	-17.84	6.13	0.63

(b) **SGFpd1**

The measure return loss is shown in Figure 5.12 below. The S₁₁ response for measurement result is slightly lower compare to simulation but it follows the pattern at the beginning frequency (0-3 GHz). At nearly 4 GHz the response for measure appear another resonance frequency reach -26 dB where in simulation only reach -10dB. But both simulation and measurement shows the resonance frequencies concentrate at higher frequency (around 7-9.5 GHz). The different between both simulation and measurement graph, maybe because of hardware imperfect condition.

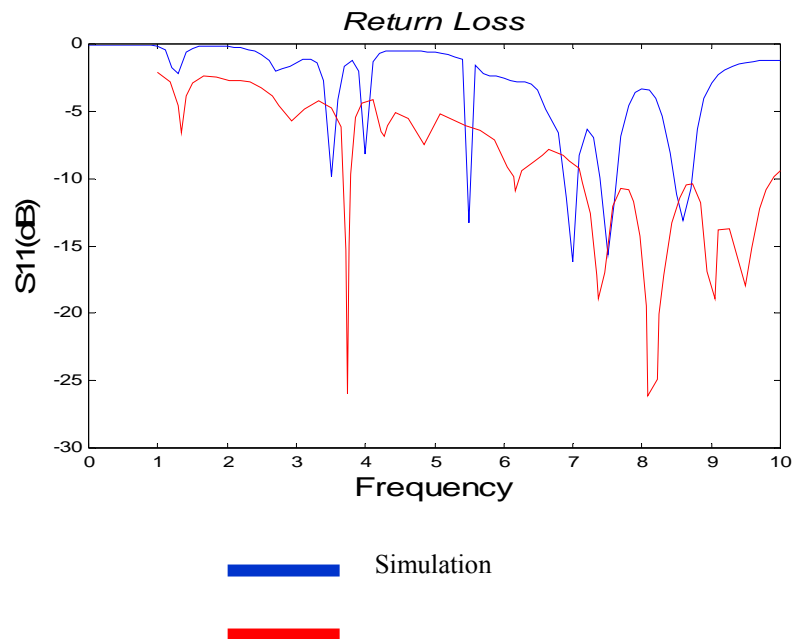


Figure 5.12: Comparison simulation and measurement of SGFpel antenna.

Table 5.8: Frequency band, return loss and bandwidth for measurement.

Band	f (GHz)	S ₁₁ (dB)	BW	f _n /f _{n+1}
m ₁	3.745	-25.95	2.4	-
m ₂	7.367	-18.5	8.86	1.97
m ₃	8.087	-26.12	11.69	1.1
m ₄	9.055	-18.95	12.92	1.12

The measures co-polarisation and cross-polarisation E-plane are presented in Figure 5.13. The cross-polarisation are lower compare than co-polarisation which are always wanted. When moving to higher resonance (second band) the main lobe become small compare to the first resonance frequency. This means the antenna gain are increasing.

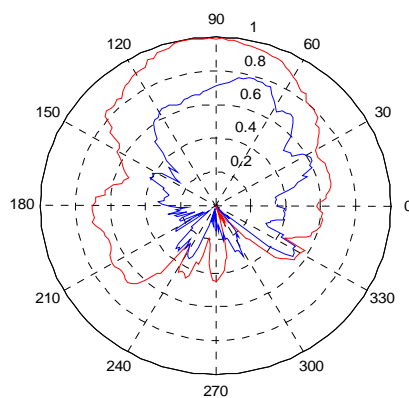

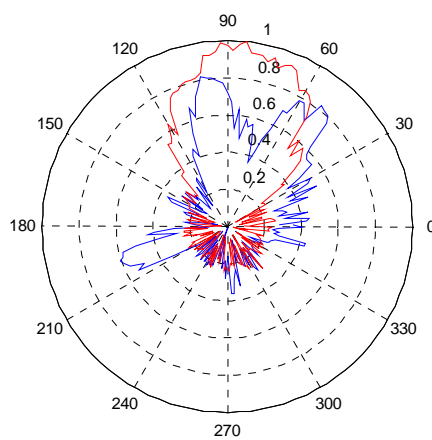
$f_1=3.745$ GHz $f_2=7.367$ GHz Cross-polar

Figure 5.13: Measurement plot of co-polarisation and cross-polarisation for SGFpd1.

(c) **SGFm1**

The SGFm1 antennas are well matched at three resonance frequency. The return loss are very good response as shown in Table 5.9. All bandwidths are better compare to Sierpinski patch antennas. The resonance frequency patterns from one band to another are nearly ≈ 2 same as the scale factor use in this monopole antenna.

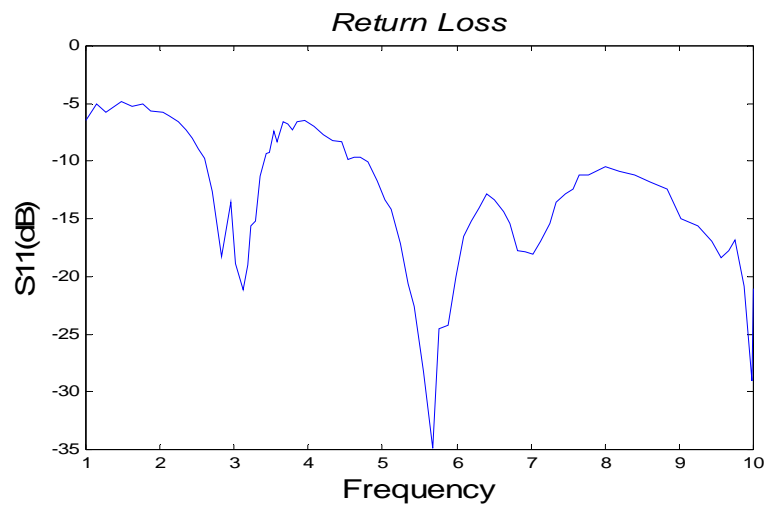


Figure 5.14: Return loss measurement for SGFm1 antenna.

Table 5.9: Frequency band, return loss and bandwidth for measurement

Band	f (GHz)	S_{11} (dB)	BW	f_n/f_{n+1}
m1	3.115	-21.14	26.74	-
m2	5.68	-34.88	57.45	1.82
m3	9.977	-29.04	16.75	1.76

The measure co-polarisation and cross-polarisation E-plane are shown in Figure 5.15. The lobes cover all 360° direction for the first resonance frequency (3.115 GHz). When move to higher resonance frequency (5.688 GHz), the lobe is divided into 4 parts. If we move to higher frequency to plotting are not consistent in reading. This is probably the high of the resonance triangle is to close too ground plane, so it effect the radiation pattern. The cross-polarisation are in good condition.

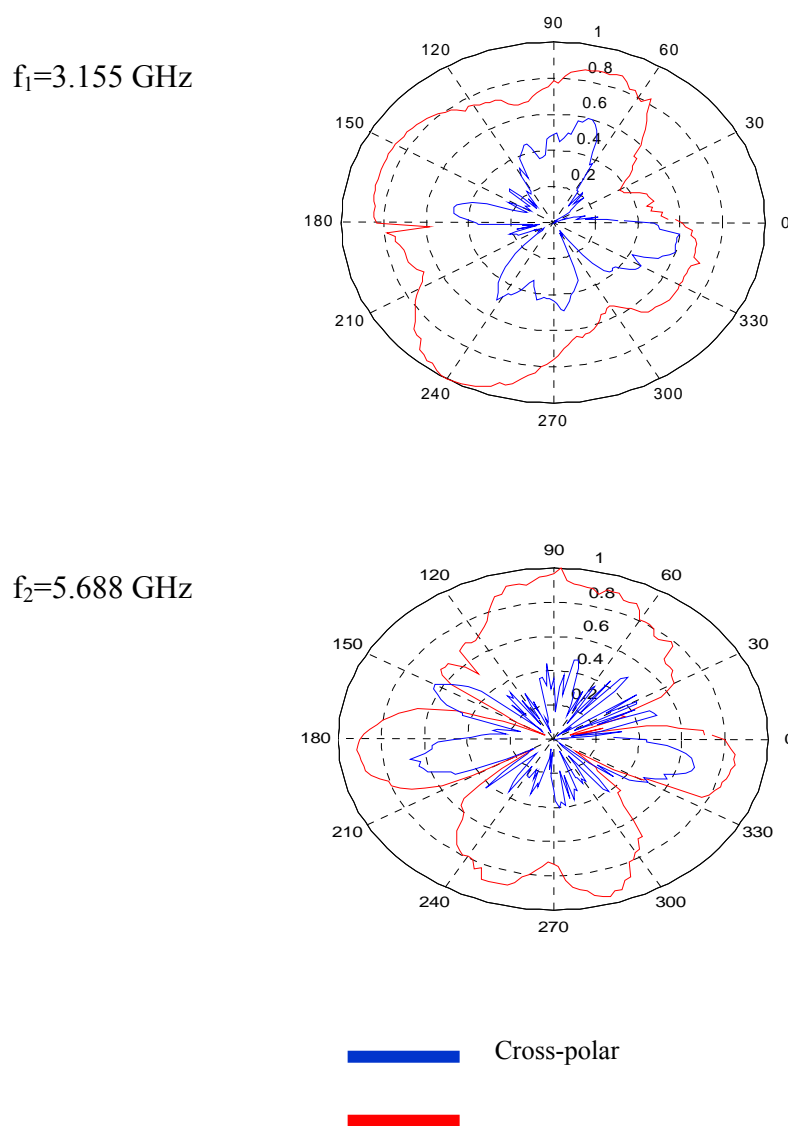


Figure 5.15: Measurement plot of co-polarisation and cross-polarisation for SGFm1

(d) **SGFm2**

Only this antenna is designed at 2.4 GHz and 5.0 GHz as mentioned before. The measurement results are in good agreement with operating frequencies that are wanted. A major improvement in bandwidth for each resonance frequency as stated in Table 5.10. Because of this antenna was designed with 3rd iteration there is 4 band of resonance frequency around <1 GHz, 2.4 GHz, 5 GHz, and 9 GHz. So each band is multiple of ≈ 2 and it agrees with the scale factor that is used for this antenna (also 2). The input impedance for each band supposedly matched near 50Ω [6]. It can't be show here because of equipment problem.

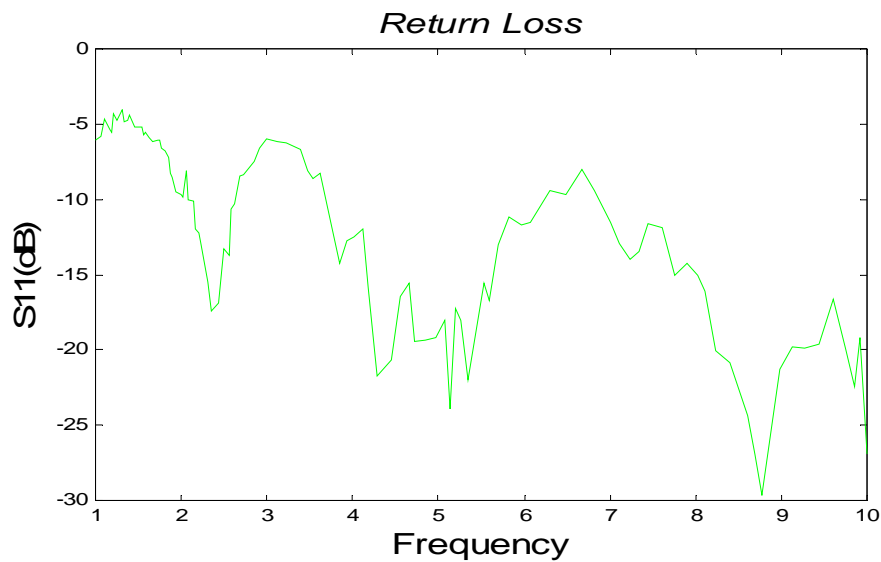


Figure 5.16: Return loss measurement for SGFm2 antenna.

Table 5.10: Frequency band, return loss and bandwidth for measurement

Band	f (GHz)	S ₁₁ (dB)	BW	f _n /f _{n+1}
m1	2.44	-16.88	19.67	-
m2	5.1	-23.91	49.42	2.09
m3	8.8	-29.66	34.09	1.73

The measure co-polarisation and cross-polarisation E-plane are shown in Figure 5.17. The lobes for the first resonance frequency (2.44 GHz) for co-polarisation have a major dip on one side. When move to higher resonance frequency (5.0 GHz), it is clear two main lobe appear on front and back of the antenna. Two small side lobe only appear both left and right of the antenna. The side lobes are small compare to previous SGFm1 antenna maybe because of larger ground plane is used for this antenna (SGFm2). The cross-polarisation are in good condition and when we move higher frequency the radiation plot of cross-polarisation become very small.

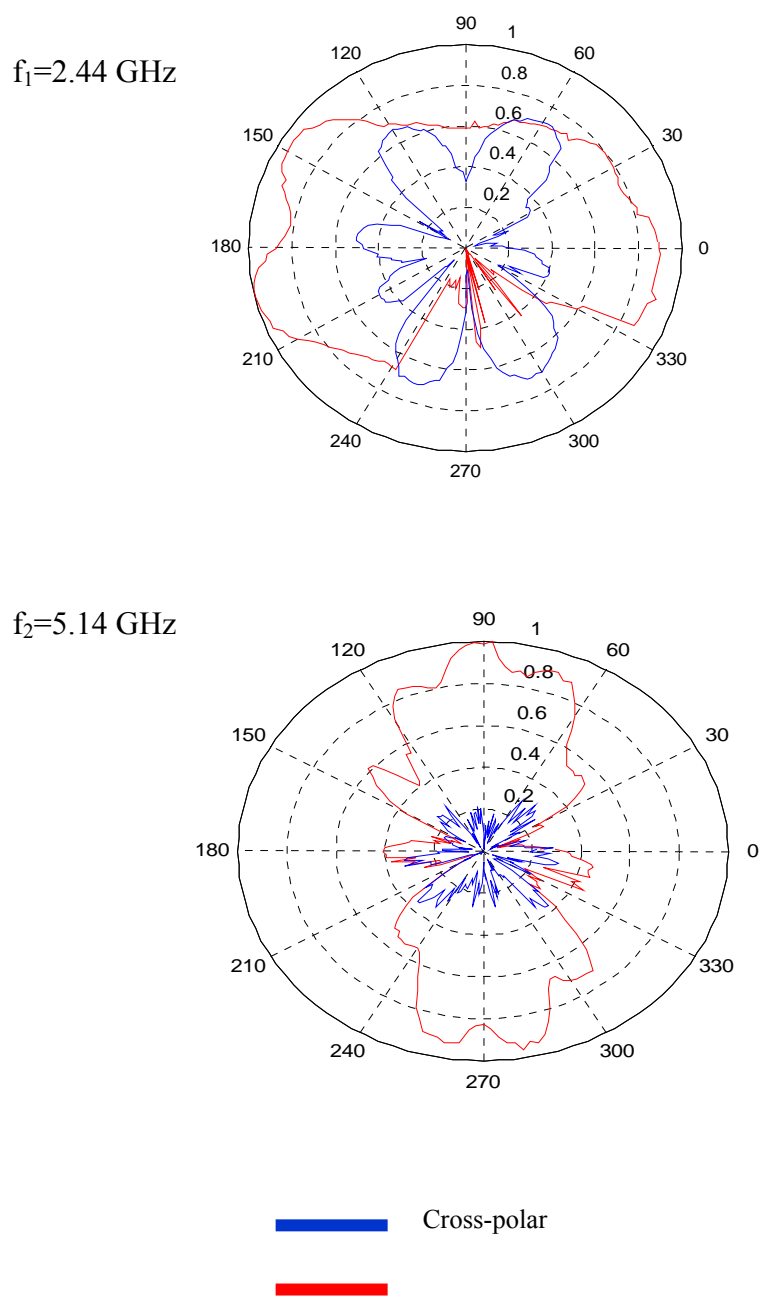


Figure 5.17: Measurement plot of co-polarisation and cross-polarisation for SGFm2.

5.3 Summary

From results it has been shown that Sierpinski gasket patch has a multiple band of resonant frequency (multiband). The band for patch type cannot be predicted. For monopole type the frequencies band is highly influenced by the geometry of Sierpinski gasket itself especially the high of each subgasket. The high of each subgasket depend on scale factor and resonant frequency. The characteristic of radiation pattern have also been study in this chapter. For monopole it can be seen that the co-polar and cross-polar introduced more side lobe at the upper band. The upper band also show characteristic ripple. This is probably the high of the resonance triangle is to close of to the ground plane.

CHAPTER 6

CONCLUSION AND RECOMMENDATIONS

6.1 Introduction

This chapter concludes the thesis. Recommendations for future work are also presented.

6.2 Conclusion

From result and discussion, it can be conclude that:

- Sierpinski gasket fractal geometry describes a multiband behavior of the fractal antenna.
- Sierpinski gasket monopole bands are log-periodically spaced by factor of two, same scale factor existing among fractal shape.

- Changing the height of each sub-gasket of Sierpinski monopole, will control the frequency band spacing and input impedance.
- The Sierpinski gasket patch antennas describe multiband frequency but the frequency band cannot be predicted.
- All band for Sierpinski gasket patch are narrowband, but with monopole type we can get wider bandwidth

6.3 Recommendations and Future Works

To further improve on the performance of this project, a few recommendations of future works suggested as follows.

- To increase the bandwidth of narrowband for Sierpinski gasket patch antenna, a multilayer or stack can be done.
- The polarization of this type of antenna can be investigated by changing the feed location and resizing two of the three side of the triangle.
- Mathematical aspects of fractal antenna can be investigate to correlate their improve characteristics.
- The gain of both Sierpinski gasket patch and monopole can be investigated. Due to delay by equipment problem, gain of these antennas cannot be measure.
- The position of ground plane for monopole type can be changed to reduce the space.

REFERENCES

- [1] D. M. Pozar, *Microwave Engineering*, New York, John Wiley & Sons, 2nd Ed. 1998.
- [2] Ramesh Garg, Prakash Bhartia, Inder Bahl, Apisak Ittiboon, *Microstrip Antenna Design Handbook*, Artech House 2001
- [3] Constantine A. Balanis, *Antenna Theory Analysis & Design*, John Wiley & Sons, 1997.
- [4] Dr E.H. Fooks, Dr R.A. Zakarevicius, *Microwave Engineering Using Microstrip Circuits*, Prentice Hall, 1991.
- [5] David M. Pozar, *Microwave And RF Design Of Wireless Systems*, John Wiley & Sons, 2001.
- [6] Carles Puente Baliarda, Jordi Romeu, Rafael Pous, Angel Cardama, *On the Behavior of the Sierpinski Multiband Fractal Antenna.*, IEEE Transaction on Antennas and Propagation, Vol 46, No 4, April 1998.
- [7] Tian Tiehong, Zhou Zheng, A Novel Multiband Antenna: Fractal Antenna, Beijing Univesity of Posts and Telecommunications, Proceedings of ICCT2003.

- [8] Douglas H. Werner and Suman Ganguly, *An Overview of Fractal Antenna Engineering Research*, IEEE Antennas and Propagation Magazine, Vol 45, No 1, February 2003.
- [9] Basil Panoutsopoulos, *Printed Circuit Fractal Antennas*, School of Science Engineering and Technology Middletown PA USA.
- [10] C. Puente, J. Romeu, R. Pous, X. Garcia and F. Benitez, *Fractal Multiband Antenna Based On The Sierpinski Gasket*, Electronics Letters 4th January 1996 Vol 32 No 1.
- [11] Carles Puente Baliarda, Jordi Romeu, Rafael Pous, Angel Cardama, *An Iterative Model fo Fractal Antennas: Application to the Sierpinski Gasket Antenna*, IEEE Transaction on Antennas and Propagation, Vol 48, No 5, 5 May 2000.
- [12] C. Borja, C. Puene and A. Medina, *Iterative Network Model to Predict the Behavior of a Sierpinski Fractal Network*, Electronics Letters 23rd July 1998 Vol 34 No 15.
- [13] C. Borja, J. Romeu, Multiband Sierpinski Fractal Patch Antenna IEEE, 2000.
- [14] B.B. Madelbrot, *The Fractal Geometry of Nature*, New York: W.H. Freeman, 1983.
- [15] Kraus John Daniel, Marhefka Ronald (2002). *Antennas: For All Applications*. 3rd Edition. New York. Mc Graw Hill
- [16] Robert A. Sainati (1996). *CAD of Microstrip for Wireless Applications*. 3rd edition. New York. McGraw Hill.
- [17] C.Puente, M.Navaro, J.Romeu, R. Paus. *Variation on The Fractal Sierpinski Antenna Flare Angle*. Electronics Letters, 1998.

- [18] C. Puente, J. Romeu, R. Bartolome. *Perturbation of Sierpinski antenna to allocate Operating Bands*. Electronics Letters, vol 32, no. 24, pp2186-2188, November 1996
- [19] Junho Yeo, Raj Mittra. *Modified Sierpinski Gasket Antenna for Multiband Applications*. IEEE Transaction on Antennas and Propagation, 2001.
- [20] Kai Chang. *Handbook of RF/Microwave Components and Engineering*. New Jersey, Wiley-Interscience.
- [21] C.T.P. Song, P.S. Hall, H. Ghafouri Shiraz, D. Wake. *Sierpinski monopole antenna with controlled band spacing and input impedance*. Electronics Letters. 24th June 1999.
- [22] P. Dehkoda, A. Tavakoli. *Circularly polarized microstrip fractal antennas*. IEEE Transaction on Antennas and Propagation. 2004.
- [23] C. Borja, J. Romeu. *Multiband Sierpinski Fractal Patch Antenna*. IEEE Transaction on Antennas and Propagation. 2000.
- [24] Hasan M. Elkamchouci, Gehan Abouelseoud. *A Compact Broadband Sierpinski Gasket Patch Microstrip Antenna*. 21st National Radio Science Conference. March 16-18, 2004.
- [25] C. Puente, J. Romeu, A. Cardama. *The Koch Monopole: A Small Fractal Antenna*. IEEE Transaction on Antennas and Propagation. Vol48, No 11, November 2000.
- [26] C. Puente, J. Anguera, E. Martinez, C. Borja, J. Soler. *Broad-band Dual Frequency Microstrip Patch Antenna With Modified Sierpinski Fractal Geometry*. IEEE Transaction on Antennas and Propagation, Vol 52, No. 1, January 2004.
- [27] K.J. Vinoy (2002). *Fractal Shaped Antenna Elements for Wide and Multiband Wireless Applications*. The Pennsylvania State University, Ph. D. Thesis.

- [28] John Gianvittorio (2000). *Fractal Antennas: Design, Characterization, and Applications*. University of California, Master Thesis.
- [29] A. Prigiobbo, M Barra A Cassinese, M Cirillo. *Superconducting resonators for telecommunication application based on fractal layout*. IOP Publishing 2004
- [30] C. Soras, M.Karaboikis, G. Tsachtsiris. *A modified Sierpinski gasket monopole antenna for a PCMCIA card operating in the 2.4 and 5.15 GHz ISM bands*. Department of Electrical and Computer Engineeing, University of Patras.
- [31] J. Anguera, C. Puente, C. Borja, R. Montero. *Bowtie Microstrip Patch Antenna based on the Sierpinski Fractal*. IEEE, 2001.
- [32] Balanis. *Antenna Teory and Design*. New York: Haeper and Row, 1982.

APPENDICES

APPENDIX A

Appendix A

Transmission lines width calculation-Mathcad2000

For given physical properties and frequency:

$$\epsilon_r := 4.5 \quad h := 1.6 \quad f := 2.5$$

For given impedance (Z_0) of single strip:

$$Z_0 := 50$$

The width over height ratio for calculated single microstrip impedance is given by:

$$d_0 := \frac{59.95\pi^2}{Z_0 \cdot \sqrt{\epsilon_r}}$$

$$H_0 := \frac{Z_0 \cdot \sqrt{2 \cdot (\epsilon_r + 1)}}{119.9} + \frac{1}{2} \left(\frac{\epsilon_r - 1}{\epsilon_r + 1} \right) \cdot \left(\ln\left(\frac{\pi}{2}\right) + \frac{1}{\epsilon_r} \cdot \ln\left(\frac{4}{\pi}\right) \right)$$

$$Z_{\text{limit}} := 44 - 2\epsilon_r$$

$$Z_{\text{limit}} = \blacksquare$$

$$U_0 := \begin{cases} \left[\left(\frac{2}{\pi} \right) \cdot (d_0 - 1) - \left(\frac{2}{\pi} \right) \cdot \ln(2 \cdot d_0 - 1) + \frac{(\epsilon_r - 1)}{\pi \cdot \epsilon_r} \cdot \left(\ln(d_0 - 1) + 0.293 - \frac{0.517}{\epsilon_r} \right) \right] & \text{if } Z_0 < Z_{\text{limit}} \\ \left[\left(\frac{e^{H_0}}{8} - \frac{1}{4 \cdot e^{H_0}} \right)^{-1} \right] & \text{if } Z_0 > Z_{\text{limit}} \end{cases}$$

$$U_0 = \blacksquare$$

$$W := U_0 \cdot h$$

$$W = \blacksquare$$

$$\epsilon_{\text{eff}} := \begin{cases} \left[\frac{\epsilon_r + 1}{2} \left[1 - \frac{1}{2 \cdot H_0} \left(\frac{\epsilon_r - 1}{\epsilon_r + 1} \right) \left(\ln\left(\frac{\pi}{2} + \frac{1}{\epsilon_r} \ln\left(\frac{4}{\pi}\right)\right) \right) \right] \right]^{-2} & \text{if } U_0 < 1.3 \\ \left[\frac{\epsilon_r + 1}{2} + \frac{\epsilon_r - 1}{2} \left(1 + \frac{10}{U_0} \right)^{-0.555} \right] & \text{if } U_0 > 1.3 \end{cases}$$

$$\epsilon_{\text{eff}} = \blacksquare$$

APPENDIX B

ResonantFrequency

$$c := 3 \cdot 10^8$$

$$h := 1.6 \cdot 10^{-3}$$

$$\epsilon_r := 4.5$$

$$m := 1$$

$$n := 0$$

$$fr := 2.5 \cdot 10^9$$

$$aeff := \frac{2 \cdot c}{3 \cdot fr \cdot \sqrt{\epsilon_r}} \cdot \sqrt{m^2 + m \cdot n + n^2}$$

$$aeff = \blacksquare$$

Guess value

$$a := 10 \cdot 10^{-2}$$

Given

$$aeff = a \cdot \left[1 + 2.199 \frac{h}{a} - 12.853 \frac{h}{a \cdot \sqrt{\epsilon_r}} + 16.436 \frac{h}{a \cdot \epsilon_r} + 6.182 \left(\frac{h}{a} \right)^2 - 9.802 \frac{1}{\sqrt{\epsilon_r}} \cdot \left(\frac{h}{a} \right)^2 \right]$$

$$newvalue := \text{Find}(a)$$

$$newvalue = \blacksquare$$

APPENDIX C

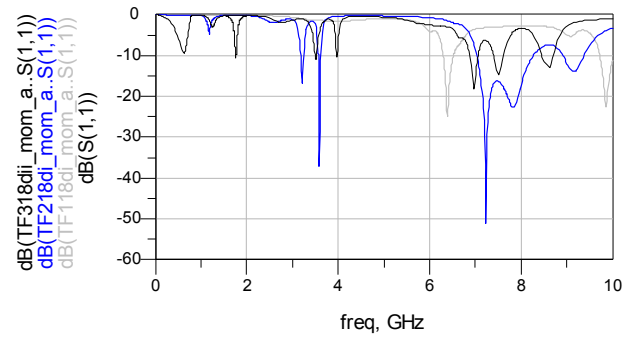


Figure 1: Return loss for SGFd1 for all iteration (simulation)

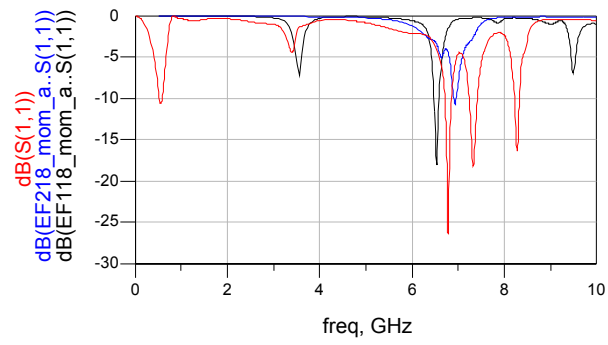


Figure 2: Return loss for SGFpe1 for all iteration (simulation)

APPENDIX D

Appendix D

Equipment for measurement and Picture of fabricated antenna.



Figure 3: UV light Equipment



Figure 4: Antenna Measurements Positioner.



Figure 5: SGFe1

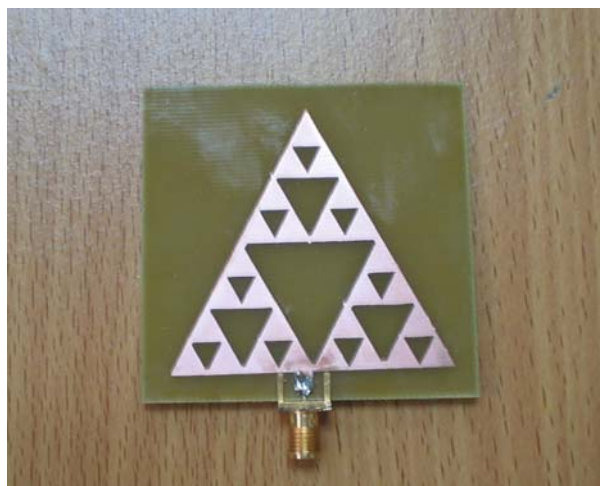


Figure 6: SGFd1

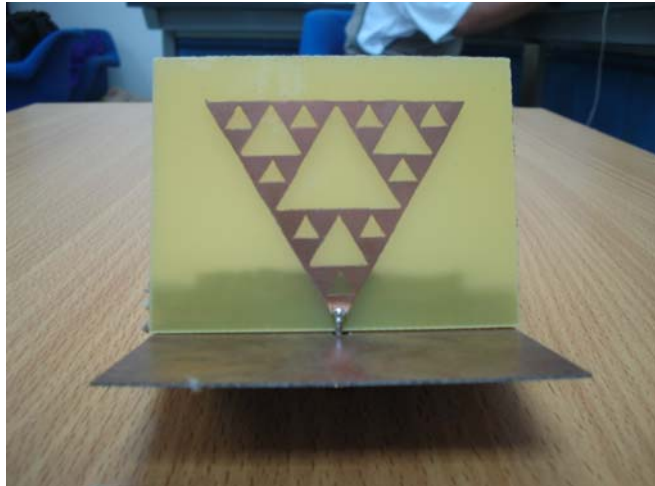


Figure 7: SGFm1



Figure 8: SGFm2

APPENDIX E

Appendix E

Example of MATLAB program to plot the radiation pattern.

```
rad1=[  
67.27  
67.77  
61.53  
63.06  
62.3  
66.13  
61.44  
61.65  
61.74  
61.41  
61.52  
62.48  
63.62  
63.9  
64.19  
65.36  
66.73  
66.34  
67.51  
68.3  
68.5  
69.21  
71.06  
69.42  
69.08  
68.46  
70.84  
67.3  
65.87  
66.03  
66.56  
62.62  
61.37
```

60.41
59.7
59.52
59.38
59.7
59.65
59.49
59.51
58.91
58.43
57.52
55.98
54.28
53.07
51.86
51.02
51.09
50.37
50.39
50.65
51.08
51.64
51.24
51.44
50.83
49.95
48.09
48.46
48.23
48.47
48.89
49.81
51.04
52.45
52.82
52.73
52.34

52.09
52.01
51.83
52.44
53.44
54.73
58.91
58.83
60.9
62.1
62.5
61.41
60.19
58.86
57.71
57.6
58.52
59.34
60.37
61.53
63.72
69.09
69.06
70.08
69
69.38
66.98
69.18
67.42
67.97
65.18
65
64.54
63.21
62.66
62.56
62.84

62.83
65.73
63.23
65.46
65.05
67.95
68.04
66.4
67.95
70.48
71.3
71.32
71.05
70.36
68.71
67.8
65.85
63.68
62.52
61.24
60.5
59.91
59.95
59.4
59.34
59.23
59.31
59.44
59.45
59.12
58.19
56.59
54.95
53.2
51.91
50.73
50.52

50.44
49.82
50.03
50.01
51.56
52.07
52.33
51.78
50.73
50.13
50.01
49.09
49.87
49.56
50.25
51.63
52.97
55.09
56.11
56.2
55.46
55.08
54.88
54.87
54.87
54.73
55.94
57.13
59.01
61.05
62.91
66.43
65.31
65.8
66.03
67.09
65.86

66.46
65.49
68.27
68.37
68.84
69.66
68.87
68.17
68.84
71.48
71.69
70.77
70.68
71.47
71.03
68.16
69.18
66.03
68.97
66.13
65.44
66.51
64.96
67.98
65.95
67.78
68.23
65.42
66.82
68.87
70.04
68.84
69.5
71.46
68.83
68.62

70.83
67.93
70.6
68.9
70.76
69.32
70.05
72.2
70.38
67.49
69.17
67.32
69.28
67.84
68
69.9
67.73
69.43
69.95
68.41
72.02
70.65
70.05
71.38
70.04
68.86
66.05
67.15
68.77
67.54
66.63
66.6
66.41
68.09
67.06
67.59
68.21

69.91
70.39
69.24
68.85
68.4
68.3
68.69
69
69.26
69.3
70.1
71.33
70.08
70.68
68.42
68.49
71.05
67.96
68.12
64.86
64.61
66.36
64.43
67.2
67.02
67.82
71.15
71.52
72.46
72.05
70.35
71.03
69.69
67.58
65.36
66.2
65.68

63.64
63.71
64.9
65.22
66.46
65.18
64.53
67.23
65.66
69.04
66.89
67.27
68.21
68.06
67.88
69.12
68.51
70.03
69.84
65.88
67.84
68.7
67.48
68.83
71.24
70.16
69.34
69.58
67.37
65.82
69.07
66.92
68.03
67.21
70.08
70.05
71.4

70.05
71.13
69.23
69.2
68.79
68.99
64.12
65.28
63.86
63.53
63.44
65.8
65.22
68.89
71.05
70.71
70.75
67.6
67.19
69.49
69.05
71.53
68.74
68.34
69.95
66.06
65.17
64.86
65.86
67.26
66.49
65.73
67.77
67.09
];

dataco=[

67.27
67.77
61.53
63.06
62.3
66.13
61.44
61.65
61.74
61.41
61.52
62.48
63.62
63.9
64.19
65.36
66.73
66.34
67.51
68.3
68.5
69.21
71.06
69.42
69.08
68.46
70.84
67.3
65.87
66.03
66.56
62.62
61.37
60.41
59.7
59.52
59.38

59.7
59.65
59.49
59.51
58.91
58.43
57.52
55.98
54.28
53.07
51.86
51.02
51.09
50.37
50.39
50.65
51.08
51.64
51.24
51.44
50.83
49.95
48.09
48.46
48.23
48.47
48.89
49.81
51.04
52.45
52.82
52.73
52.34
52.09
52.01
51.83
52.44

53.44
54.73
58.91
58.83
60.9
62.1
62.5
61.41
60.19
58.86
57.71
57.6
58.52
59.34
60.37
61.53
63.72
69.09
69.06
70.08
69
69.38
66.98
69.18
67.42
67.97
65.18
65
64.54
63.21
62.66
62.56
62.84
62.83
65.73
63.23
65.46

65.05
67.95
68.04
66.4
67.95
70.48
71.3
71.32
71.05
70.36
68.71
67.8
65.85
63.68
62.52
61.24
60.5
59.91
59.95
59.4
59.34
59.23
59.31
59.44
59.45
59.12
58.19
56.59
54.95
53.2
51.91
50.73
50.52
50.44
49.82
50.03
50.01

51.56
52.07
52.33
51.78
50.73
50.13
50.01
49.09
49.87
49.56
50.25
51.63
52.97
55.09
56.11
56.2
55.46
55.08
54.88
54.87
54.87
54.73
55.94
57.13
59.01
61.05
62.91
66.43
65.31
65.8
66.03
67.09
65.86
];

datacross=[
66.46

65.49
68.27
68.37
68.84
69.66
68.87
68.17
68.84
71.48
71.69
70.77
70.68
71.47
71.03
68.16
69.18
66.03
68.97
66.13
65.44
66.51
64.96
67.98
65.95
67.78
68.23
65.42
66.82
68.87
70.04
68.84
69.5
71.46
68.83
68.62
70.83
67.93

70.6
68.9
70.76
69.32
70.05
72.2
70.38
67.49
69.17
67.32
69.28
67.84
68
69.9
67.73
69.43
69.95
68.41
72.02
70.65
70.05
71.38
70.04
68.86
66.05
67.15
68.77
67.54
66.63
66.6
66.41
68.09
67.06
67.59
68.21
69.91
70.39

69.24
68.85
68.4
68.3
68.69
69
69.26
69.3
70.1
71.33
70.08
70.68
68.42
68.49
71.05
67.96
68.12
64.86
64.61
66.36
64.43
67.2
67.02
67.82
71.15
71.52
72.46
72.05
70.35
71.03
69.69
67.58
65.36
66.2
65.68
63.64
63.71

64.9
65.22
66.46
65.18
64.53
67.23
65.66
69.04
66.89
67.27
68.21
68.06
67.88
69.12
68.51
70.03
69.84
65.88
67.84
68.7
67.48
68.83
71.24
70.16
69.34
69.58
67.37
65.82
69.07
66.92
68.03
67.21
70.08
70.05
71.4
70.05
71.13

69.23
69.2
68.79
68.99
64.12
65.28
63.86
63.53
63.44
65.8
65.22
68.89
71.05
70.71
70.75
67.6
67.19
69.49
69.05
71.53
68.74
68.34
69.95
66.06
65.17
64.86
65.86
67.26
66.49
65.73
67.77
67.09
];

radl=(radl)*(-1);

dataco=(dataco)*(-1);

```
datacross=(datacross)*(-1);
ref1=min(rad1);
ref2=max(rad1)-ref1;
ref3=max(dataco)-ref1;
ref4=max(datacross)-ref1;

for i=1:length(dataco)
    rad2=dataco(i,1)-ref1;
    ang=2*i*pi/180;

    r1=rad1(i,1);
    plo1(i,1)=ang;
    plo1(i,2)=rad2/ref2;
end

for j=1:length(datacross)
    rad3=datacross(j,1)-ref1;

    r1=rad1(i,1);
    plo2(j,2)=rad3/ref2;
end

polar(plo1(:,1),plo1(:,2),'r');
hold
polar(plo1(:,1),plo2(:,2));
```